XII

Baryon properties

An important sector of hadron phenomenology is associated with the electroweak interactions. Baryons provide a particularly rich source of information, with data on vector and axial-vector couplings, magnetic moments, and charge radii. In Sect. XII–1, we describe the procedure for computing matrix elements in the constituent quark model, and then turn to a variety of applications in the succeeding sections.[1]

XII–1 Matrix-element computations

Much of the application of the quark model to physical systems involves the calculation of matrix elements. The subject divides naturally into two parts. On the one hand, many quantities of interest follow from just the flavor and spin content of the hadronic states. On the other, it is often necessary to have a detailed picture of the quark spatial wavefunction.

Flavor and spin matrix elements

For the first of these, the quark model is particularly appealing because of the intuitive physical picture which it provides. For example, consider the quark content of the proton state vector, which we reproduce here from Table XI–2,

$$|p_\uparrow\rangle = \frac{1}{\sqrt{18}}\epsilon_{ijk}[(u_{i\downarrow}^\dagger d_{j\uparrow}^\dagger - u_{i\uparrow}^\dagger d_{j\downarrow}^\dagger)u_{k\uparrow}^\dagger]\,|0\rangle. \tag{1.1}$$

The first two quarks form a spin-zero, isospin-zero pair with the net spin and isospin of the proton being given by the final quark. The prefactor of $1/\sqrt{18}$ ensures that the state vector has unit normalization. Calculation reveals that one-third of the magnitude of this normalization factor comes from the $u_\uparrow u_\downarrow d_\uparrow$ term

---

[1] The reader can also consult the $N_c \to \infty$ studies as described in [DaJM 94, Je 98].

330

Table XII–1. *Some baryon octet expectation values.*

	p	n	Λ	Σ^+	Σ^0	Σ^-	Ξ^0	Ξ^-
$\langle Q \rangle$	1	0	0	1	0	-1	0	-1
$\langle Q\sigma_z \rangle$	1	$-2/3$	$-1/3$	1	$1/3^a$	$-1/3$	$-2/3$	$-1/3$
$\langle \lambda_3\sigma_z \rangle$	$5/3$	$-5/3$	$2/\sqrt{6}$	$4/3$	0	$-4/3$	$-1/3$	$1/3$

^{a}The off-diagonal transition $\Sigma^0 \to \Lambda$ has $|\langle Q\sigma_z \rangle| = 1/\sqrt{3}$.

and two-thirds from the $u_\uparrow u_\uparrow d_\downarrow$ term, i.e. one concludes that 'the proton is twice as likely to be found in the configuration with the u-quark spins aligned than anti-aligned',

$$\text{Prob.} = \begin{cases} 2/3 & (u_\uparrow u_\uparrow d_\downarrow), \\ 1/3 & (u_\uparrow u_\downarrow d_\uparrow). \end{cases} \tag{1.2}$$

The 'six parts in eighteen' of the $u_\uparrow u_\downarrow d_\uparrow$ configuration arises entirely from the six ways that color can be distributed among three distinct entities. The configuration $u_\uparrow u_\uparrow d_\downarrow$ is twice as large due to the presence of two $u_\uparrow$ states. Similar kinds of inferences can be drawn for the remaining baryon state vectors in Table XI–2.

We can proceed analogously in deriving and interpreting various matrix-element relationships. It is instructive to work at first in the limit of $SU(3)$ invariance because more predictions become available. The effect of symmetry breaking is addressed in Sect. XII–2. Let us consider matrix elements, taken between members of the spin one-half baryon octet, of the operators

$$\text{squared charge-radius}: \int d^3x\, r^2 \psi^\dagger Q \psi \qquad \propto \langle Q \rangle,$$

$$\text{axial-vector current}: \int d^3x\, \psi^\dagger \gamma_3\gamma_5\lambda_3 \psi \qquad \propto \langle \lambda_3\sigma_z \rangle,$$

$$\text{magnetic moment}: \int d^3x\, \frac{1}{2}(\mathbf{r} \times \psi^\dagger \boldsymbol{\alpha} Q \psi)_3 \qquad \propto \langle Q\sigma_z \rangle. \tag{1.3}$$

Along with the definition of each operator is indicated the flavor–spin attribute of an individual quark which is being averaged over. For example, a magnetic moment is sensitive to the combination $Q\sigma_z$ of each quark within the baryon. Matrix elements will then be products of such averages times quark wavefunction overlap integrals. The flavor–spin averages for the baryon octet are displayed in Table XII–1.

To see how these values are arrived at, let us compute the value $5/3$ obtained for the proton axial-vector matrix element. For the configuration $u_\uparrow u_\uparrow d_\downarrow$, which occurs with a probability of $2/3$, the average value of $\lambda_3\sigma_z$ equals $(1 + 1 + 1) \times 2/3 = 2$,

whereas for the configuration $u_\uparrow u_\downarrow d_\uparrow$ one finds $(1-1-1) \times 1/3 = -1/3$. Together they sum to the value $5/3$.

Overlaps of spatial wavefunctions

The spatial description of quark wavefunctions is less well understood than the spin/flavor aspect of the phenomenology.[2] The most extensive studies of the spatial wavefunctions are associated with matrix elements of *currents*. Because these are bilinear in quark fields and because of the wavefunction normalization condition, the magnitudes of these amplitudes are constrained to be nearly correct. Dimensional matrix elements are primarily governed by the *radius* of the bound state. As long as the proper value is fed into the calculation, the scale should come out right.

As noted in Sect. XI–1, a relativistic quark moving in a spin-independent central potential has a ground-state wavefunction of the form

$$\psi(\mathbf{x})\Big|_{\text{gnd}} = \begin{pmatrix} i\, u(r)\, \chi \\ \ell(r)\boldsymbol{\sigma} \cdot \hat{\mathbf{x}}\, \chi \end{pmatrix} e^{-iEt}, \tag{1.4}$$

where u, ℓ signify 'upper' and 'lower' components. For the bag model, these radial wavefunctions are just spherical Bessel functions. This form also appears in some relativistic harmonic oscillator models, which use a central potential. To characterize different types of relativistic behavior, it is worthwhile to express matrix elements in terms of u and ℓ without specifying them in detail. The normalization condition for the spatial wavefunction is then

$$\int d^3x \; \psi^\dagger(\mathbf{x})\psi(\mathbf{x}) = \int d^3x \; (u^2(r) + \ell^2(r)) = 1. \tag{1.5}$$

In the nonrelativistic regime, the lower component vanishes ($\ell = 0$).

Let us consider the size of the lower components which occur in various approaches. In the bag model one obtains for massless quarks the integrated value

$$\int d^3x \; \ell^2(r) \simeq 0.26. \tag{1.6}$$

Relativistic effects are often included in potential models by working in momentum space and employing the spinor appropriate for a quark q in momentum eigenstate $\mathbf{p}$,

---

[2] Even the *experimental* value of the proton charge radius r_{E} is in question. The historical approach, to measure the differential cross section in elastic electron–proton scattering at low Q^2, gives $r_{\text{E}} = 0.879(8)$ fm and $r_{\text{E}} = 0.875(11)$ fm [Zh *et al.* 11] in recent experiments. By contrast, measurement of the $2S_{1/2}^{F=0} - 2P_{3/2}^{F=1}$ energy difference in muonic hydrogen [An *et al.* 13] yields (using a consistent definition of charge radius) $r_{\text{E}} = 0.84087(39)$ fm, which is at 7σ variance relative to the scattering value.

$$u(\mathbf{p}) = \sqrt{E + m_q} \begin{pmatrix} \chi \\ \dfrac{\boldsymbol{\sigma} \cdot \mathbf{p}}{E + m_q} \chi \end{pmatrix}. \tag{1.7}$$

In this case the relevant prescription is

$$\int d^3x \, \ell^2(r) \rightarrow \left\langle \frac{\mathbf{p}^2}{2E(E + m_q)} \right\rangle, \tag{1.8}$$

where the averaging is taken over the momentum-space wavefunction of the particular model. Using the uncertainty principle relation of Eq. (XI–1.14) to estimate $\langle \mathbf{p}^2 \rangle$, we find typical values

$$\left\langle \frac{\mathbf{p}^2}{2E(E + m_q)} \right\rangle \simeq 0.13 \rightarrow 0.20 \tag{1.9}$$

for a confinement scale of 1 fm. Larger effects are found in the harmonic-oscillator model if one uses the value $\alpha^2 = 0.17 \text{ GeV}^2$ (see Fig. XI–2). Generally, the lower component is found to be significant but not dominant in quark wavefunctions.

Connection to momentum eigenstates

In all cases except for the nonrelativistic version of the harmonic oscillator model, one cannot explicitly separate out the center-of-mass motion. The result of a quark model description of a bound state is a configuration localized in coordinate space, i.e., a position eigenstate. However, the analysis of scattering and decay deals with the plane waves of momentum eigenstates.

   The basic assumption made in all quark models is that the bound state with a given set of quantum numbers is related to only those momentum eigenstates of the same type. If we denote $|H(\mathbf{x})\rangle$ as a unit-normalized hadron state centered about point $\mathbf{x}$ and $|H(\mathbf{p})\rangle$ as a plane-wave state, then we have

$$|H(\mathbf{x})\rangle = \int d^3p \, \varphi(\mathbf{p}) e^{i\mathbf{p}\cdot\mathbf{x}} |H(\mathbf{p})\rangle. \tag{1.10}$$

We shall give a prescription for obtaining a functional form for $\varphi(\mathbf{p})$ shortly. Let us normalize the plane-wave states for both mesons and baryons as

$$\langle H(\mathbf{p}')|H(\mathbf{p})\rangle = 2\omega_{\mathbf{p}} (2\pi)^3 \delta^{(3)}(\mathbf{p}' - \mathbf{p}). \tag{1.11}$$

The constraint of unit normalization then implies

$$\int d^3p \, 2\omega_{\mathbf{p}} (2\pi)^3 |\varphi(\mathbf{p})|^2 = 1. \tag{1.12}$$

We can employ the above wavepacket description to derive a general procedure within the quark model for calculating matrix elements [DoJ 80]. Many matrix elements of interest involve a local operator O evaluated between initial and final single-hadron states. Let us characterize the magnitude of the matrix element in terms of a constant g. Then, for baryons in the momentum basis, the spatial dependence is given by

$$\langle B'(\mathbf{p}') \,|O(x)|\, B(\mathbf{p}) \rangle = g \, \overline{u}(\mathbf{p}')\Gamma_O u(\mathbf{p}) \, e^{i(p'-p)\cdot x}, \qquad (1.13)$$

where Γ_O is a Dirac matrix appropriate for the operator O. By comparison, one obtains in any bound-state quark model (QM) calculation a spatial dependence whose specific form is model-dependent,

$$_{\mathrm{QM}}\langle B' \,|O(x)|\, B \rangle_{\mathrm{QM}} = f(x). \qquad (1.14)$$

Hereafter, let us center all quark model states at the origin. The method of wavepackets then implies

$$_{\mathrm{QM}}\langle B'| \int d^3x \; O(x)|B\rangle_{\mathrm{QM}} = g \int d^3x \int d^3p' d^3p \; \varphi^*(\mathbf{p}')\varphi(\mathbf{p})$$
$$\times \overline{u}(\mathbf{p}')\Gamma_O u(\mathbf{p})e^{i(p'-p)\cdot x}$$
$$= g \int d^3p \; (2\pi)^3 \, |\varphi(\mathbf{p})|^2 \, \overline{u}(\mathbf{p})\Gamma_O u(\mathbf{p}). \qquad (1.15)$$

For sufficiently heavy bound states the fluctuation in squared momentum $\langle \mathbf{p}^2 \rangle$ is small, and one may expand about $|\mathbf{p}| = 0$,

$$\overline{u}(\mathbf{p})\Gamma_O u(\mathbf{p}) = \overline{u}(\mathbf{0})\Gamma_O u(\mathbf{0}) + \mathcal{O}\left(\langle \mathbf{p}^2 \rangle/m_B^2\right). \qquad (1.16)$$

A common approach consists of keeping only the leading term to obtain

$$\frac{g}{2m_B} \, \overline{u}(\mathbf{0})\Gamma_O u(\mathbf{0}) = \; _{\mathrm{QM}}\langle B'| \int d^3x \; O(x) \,|B\rangle_{\mathrm{QM}}. \qquad (1.17)$$

It is interesting to note that this relation, often thought of as fundamental, is in fact only an approximation.

As an example, let us perform the complete quark model procedure for the neutron–proton axial-vector current matrix element. We begin by defining as usual

$$\langle p(\mathbf{p}_2, s_2) \,\big|A_\mu(x)\big|\, n(\mathbf{p}_1, s_1) \rangle = g_{\mathrm{A}}\overline{u}(\mathbf{p}_2, s_2)\gamma_\mu\gamma_5 u(\mathbf{p}_1, s_1)e^{i(p_2-p_1)\cdot x} + \cdots . \qquad (1.18)$$

For spin-up nucleons the choice $\mu = 3$ gives

$$\overline{u}(\mathbf{0}, \uparrow)\gamma_3\gamma_5 u(\mathbf{0}, \uparrow) = 2m_N, \qquad (1.19)$$

yielding for Eq. (1.18) the basic formula,

$$g_A = {}_{\text{QM}}\langle p_\uparrow | \int d^3x \, \overline{u}(x)\gamma_3\gamma_5 d(x) \, |n_\uparrow\rangle_{\text{QM}}. \tag{1.20}$$

The field operator for any quark q is expanded as in Eq. (XI–1.1),

$$q_\alpha(x) = \sum_{n,s} \left[\psi_{n,s}(x)e^{-i\omega_n t} q_{n,\alpha}(s) + \psi_{\overline{n},\overline{s}}(x)e^{i\omega_{\overline{n}}t}\overline{q}^{\dagger}_{\overline{n},\alpha}(\overline{s}) \right]. \tag{1.21}$$

Substituting, we have

$$g_A = {}_{\text{QM}}\langle p_\uparrow | \int d^3x \, \overline{\psi}_{0,s'}(x) \, \gamma_3\gamma_5 \psi_{0,s}(x) \, u^{\dagger}_{\alpha}(s)d_\alpha(s')|n_\uparrow\rangle_{\text{QM}}, \tag{1.22}$$

where only the $n = 0$ ground-state mode contributes. At this stage, one can factor-ize the spin and space components by using the general ground-state wavefunction of Eq. (1.4). This leads to

$$\int d^3x \, \overline{\psi}_{0,s}\gamma_3\gamma_5\psi_{0,s'} = \int d^3x \, \chi^{\dagger}_s(u^2\sigma_3 - \ell^2\hat{\mathbf{r}}_3\boldsymbol{\sigma}\cdot\hat{\mathbf{r}})\chi_{s'}$$
$$= \sigma_3^{ss'} \int d^3x \, (u^2 - \frac{1}{3}\ell^2), \tag{1.23}$$

and thus

$$g_A = \int d^3x \, \left(u^2 - \frac{1}{3}\ell^2 \right) {}_{\text{QM}}\langle p_\uparrow \left| u^{\dagger}(s,\alpha)\sigma_3^{ss'}d(s',\alpha) \right| n_\uparrow\rangle_{\text{QM}}. \tag{1.24}$$

Finally, upon dealing with the spin dependence in Eq. (1.24), we obtain

$$g_A = \frac{5}{3} \int d^3x \, \left(u^2 - \frac{1}{3}\ell^2 \right) = \frac{5}{3} \left(1 - \frac{4}{3} \int d^3x \, \ell^2 \right). \tag{1.25}$$

Any nonrelativistic quark model, having zero lower components, would simply yield $g_A = 5/3$. If one desires to make relativistic corrections to such a model, the result can be inferred from the above general formula with the appropriate substitution of Eq. (1.8). Clearly, the procedure just given can be extended to matrix elements of any physical observable.

The wavepacket formalism also allows for the estimation of the 'center-of-mass' correction. This arises from the $\langle \mathbf{p}^2 \rangle$ modifications to Eq. (1.16). For the axial cur-rent, the zero-momentum relation in Eq. (1.19) is extended for nonzero momentum to

$$\frac{\overline{u}_2(\mathbf{p},\uparrow)\gamma_3\gamma_5 u_1(\mathbf{p},\uparrow)}{2E} = 1 - \frac{\mathbf{p}^2}{3m_1 m_2} \left(\frac{1}{4} + \frac{3}{8}\frac{m_2}{m_1} + \frac{3}{8}\frac{m_1}{m_2} \right) + \mathcal{O}(\mathbf{p}^4), \tag{1.26}$$

where an average over the direction of **p** has been performed. This expression generalizes Eq. (1.25) to

$$g_A \left[1 - \frac{\langle \mathbf{p}^2 \rangle_{np}}{3 m_n m_p} \left(\frac{1}{4} + \frac{3}{8} \frac{m_p}{m_n} + \frac{3}{8} \frac{m_n}{m_p} \right) \right] = \frac{5}{3} \int d^3 x \left(u^2 - \frac{1}{3} \ell^2 \right), \quad (1.27)$$

where $\langle \mathbf{p}^2 \rangle_{np} \simeq 0.5 \text{ GeV}^2$ is a typical bag model value.

It is possible to argue that in the transition from the current quarks of the *QCD* lagrangian to the constituent quarks of the quark model, the couplings to currents should be modified. For example, one might suspect that the coupling of a constituent quark to the axial current occurs not with strength unity, but with a strength $g_A^{(q)}$ such that the nonrelativistic expectation is not $g_1 = 5/3$ but rather $g_1 = 5 g_A^{(q)}/3$. The choice $g_A^{(q)} \simeq 3/4$ would then yield the experimental value. This is not unreasonable but, if fully adopted, leads to a lack of predictivity. In such a picture, not only can the magnetic moments and weak couplings be renormalized, but also the spin and flavor structures. That is, in the 'dressing' process which a constituent quark undergoes, there could be 'sea' quarks, such that the constituent u quark could have gluonic, d-quark, or s-quark content. Likewise, some of the spin of the constituent quarks could be carried by gluons. One is then at a loss to know how to calculate matrix elements of currents. In practice, however, the naive quark model, with no rescaling of g_A or of the magnetic moment, does a reasonable job of describing current matrix elements. It is then of interest to study both the structure and limitations of this simple approach.

Calculations in the Skyrme model

There are several differences between taking matrix elements in the quark model and in the Skyrme model [Sk 62]. To begin, in the quark model a current is expressed in terms of a bilinear covariant in the quark fields (cf. Eq. (1.3)), whereas in the Skyrme model the representation of a current is rather different. As an example, application of either Noether's theorem or the external source method of Sect. IV–6 identifies the $SU(2)$ vector and axial-vector currents to be

$$\left(J_{\substack{v \\ a}} \right)_\mu^a = \frac{i F_\pi^2}{4} \text{Tr} \left(\tau^a (\partial_\mu U \, U^\dagger \pm \partial_\mu U^\dagger \, U) \right)$$

$$- \frac{i}{16 e^2} \Big[\text{Tr} \left([\tau^a, \partial_\nu U \, U^\dagger][\partial_\mu U \, U^\dagger, \partial^\nu U \, U^\dagger] \right)$$

$$\pm \text{Tr} \left([\tau^a, \partial_\nu U^\dagger \, U][\partial_\mu U^\dagger \, U, \partial^\nu U^\dagger \, U] \right) \Big], \quad (1.28)$$

where $U = A(t) U_0 A^{-1}(t)$ is the quantized skyrmion form and $A(t)$ is an $SU(2)$ matrix. We shall neglect derivatives of $A(t)$, as the quantization hypothesis corresponds to slow rotations. This leads to a result similar in form to Eq. (1.28), but

with $U \to U_0$ and $\tau^a \to A^{-1}(t)\tau^a A(t)$. The answer may be simplified by use of the explicit form of U_0 appearing in Eq. (XI–4.15).

Let us use Eq. (1.28) to compute the spatial integral of the axial current. After some algebra, we obtain a product of spatial and internal factors,

$$\int d^3x \, (J_A)^a_j = -G_5 \, \text{Tr} \, (\tau^a A \tau^j A^{-1}),$$

$$G_5 = -\frac{\pi}{3e^2} \int_0^\infty d\tilde{r} \, \tilde{r}^2 \left[F' + \frac{\sin 2F}{\tilde{r}} + \frac{4 \sin 2F}{\tilde{r}} (F')^2 \right.$$
$$\left. + \frac{8 \sin^2 F}{\tilde{r}^2} F' + \frac{4 \sin^2 F \, \sin 2F}{\tilde{r}^3} \right], \tag{1.29}$$

where a is the isospin component and j is the Lorentz component. This is now suitable for taking matrix elements, such as

$$\langle p_\uparrow | \int d^3x \, (J_A)^a_j \, |p_\uparrow\rangle = \int d^3x \int d\Omega_3 \, \langle p_\uparrow | A \rangle \, (J_A)^a_j \, \langle A | p_\uparrow \rangle$$

$$= G_5 \int d\Omega_3 \, D^{(\frac{1}{2})*}_{-\frac{1}{2},\frac{1}{2}}(A) \, \text{Tr} \, (\tau^a A \tau^j A^{-1}) D^{(\frac{1}{2})}_{-\frac{1}{2},\frac{1}{2}}(A), \tag{1.30}$$

where we have used the completeness relation of Eq. (XI–4.42). Upon expressing the trace in Eq. (1.30) as a rotation matrix, $\text{Tr} \, (\tau^k A \tau^l A^{-1})/2 = D^{(1)}_{kl}$, we can determine the group integration in Eq. (1.30) in terms of $SU(2)$ Clebsch–Gordan coefficients,

$$\int d\Omega_3 \, D^{(T'')*}_{mn}(A) D^{(T')}_{kl}(A) D^{(T)}_{ij}(A) = (-)^{2(T'-T+m)} \frac{2\pi^2}{2T''+1} C^{T'TT''}_{kim} C^{T'TT''}_{ljn}. \tag{1.31}$$

Alternatively, one can work directly with the collective coordinates, e.g., with the aid of Eqs. (XI–4.41–4.44) we obtain for $a = j = 3$

$$-\frac{2G_5}{\pi^2} \int d\Omega_3 \, (a_1 - ia_2)(a_0^2 + a_3^2 - a_1^2 - a_2^2)(a_1 + ia_2) = \frac{2}{3} G_5. \tag{1.32}$$

Before one can infer a Skyrme model prediction for g_A from this calculation, there is a subtlety not present for the quark calculation, which must be addressed. Due to the original chirally invariant lagrangian, the Skyrme model is unique among phenomenological models in being completely compatible with the constraints of chiral symmetry. As a consequence, the near-static axial-vector matrix element is constrained to obey

$$q_j \langle p(\mathbf{p'})|(J_A)^3_j|p(\mathbf{p})\rangle = 0, \qquad (q = p - p') \tag{1.33a}$$

and hence must be of the form [AdNW 83],

$$\langle p(\mathbf{p}')|(J_A)^3_j|p(\mathbf{p})\rangle = 2m_p g_\mathrm{A} \left(\delta_{jk} - \frac{q_j q_k}{|\mathbf{q}|^2}\right)\langle\sigma_k\rangle. \qquad (1.33\mathrm{b})$$

The term containing $|\mathbf{q}|^{-2}$ arises from the pion pole, as will be discussed in Sect. XII–3 in connection with the Goldberger–Treiman relation. An angular average of Eq. (1.33b) then yields $2g_\mathrm{A}/3$, which from comparison with Eq. (1.32) implies $g_\mathrm{A} = G_5$. Thus in the Skyrme model, the axial-vector coupling constant equals the radial integral in Eq. (1.29) which defines G_5. Use of the profile given in Sect. XI–4 leads to the prediction $g_\mathrm{A} = 0.61$, which is about only one-half the experimental value and constitutes a well-known deficiency of skyrmion phenomenology. Presumably, consideration of a more general chiral lagrangian could modify this result by including higher derivative components in the weak current.

Pions may be added to the Skyrme description through introduction of the matrix ξ described in App. B–4 [Sc 84],

$$U = \xi A(t) U_0 A^{-1}(t)\xi, \qquad \xi = \exp\left[i\boldsymbol{\tau}\cdot\boldsymbol{\pi}/(2F_\pi)\right]. \qquad (1.34)$$

If currents are formed using this ansatz, some terms occur without derivatives on the pion field, while others contain one or more factors of $\partial^\mu\pi$. Since $\partial^\mu\pi$ gives rise to a momentum factor q^μ_π when matrix elements are taken and soft-pion theorems deal with the limit $q^\mu_\pi \to 0$, the lowest-order soft-pion contribution will consist of keeping only terms without derivatives. Thus in the process $\nu_\mu + N \to N + \pi + \mu$ the final-state pion is produced by a hadronic weak current and the soft-pion theorem relates the $N \to N\pi$ matrix element to the $N \to N$ current form factors. Expanding the currents to first order in the pion field yields

$$\left(J_\mathrm{v}_\mathrm{a}\right)^a_\mu = \frac{iF_\pi}{2}\left[\mathrm{Tr}\left(\tau^a A^{-1}\left(\partial_\mu U_0^\dagger\, U_0 \pm \partial_\mu U_0\, U_0^\dagger\right)A\right)\right.$$
$$\left. - \frac{i\pi^b}{2F_\pi}\mathrm{Tr}\left([\tau^a,\tau^b]A^{-1}\left(\partial_\mu U_0^\dagger\, U_0 \mp \partial_\mu U_0\, U_0^\dagger\right)A\right) + \cdots\right], \quad (1.35)$$

where for notational simplicity we have displayed only the first term in the current. Note the sign flip in the second line. This form is in accord with the soft-pion theorem (see App. B–3)

$$\lim_{q^\lambda_\pi \to 0}\langle N'(\mathbf{p}')\pi^b(\mathbf{q}_\pi)|\left(J_\mathrm{v}_\mathrm{a}\right)^a_\mu|N(\mathbf{p})\rangle = -\frac{i}{F_\pi}\langle N'(\mathbf{p}')|\left[Q^b_5,\left(J_\mathrm{v}_\mathrm{a}\right)^a_\mu\right]|N(\mathbf{p})\rangle$$
$$= -\frac{\epsilon^{abc}}{F_\pi}\langle N'(\mathbf{p}')|\left(J_\mathrm{v}_\mathrm{a}\right)^c_\mu|N(\mathbf{p})\rangle, \qquad (1.36)$$

where the current commutation rules of App. B–3 have been used.

XII–2 Electroweak matrix elements

The static properties of baryons can be determined from their coupling to the weak and electromagnetic currents. In this section, we shall describe these features in terms of the quark model.

Magnetic moments

The generic quark model assumption for the magnetic moment is that the individual quarks couple independently to a photon probe. For ground-state baryons where all the quarks move in relative S waves, the magnetic moment is thus the vector sum of the quark magnetic moments,

$$\boldsymbol{\mu}_{\text{baryon}} = \sum_{i=1}^{3} \mu_i \boldsymbol{\sigma}_i, \tag{2.1}$$

where $\boldsymbol{\sigma}_i$ is the Pauli matrix representing the spin state of the ith quark and μ_i is the magnitude of the quark magnetic moment.[3] Since the light hadrons contain three quark flavors, the most general fitting procedure to the moments of the baryon octet will involve the magnetic moments μ_u, μ_d, μ_s.

It is straightforward to infer baryon magnetic-moment predictions in the quark model directly from the state vectors of Table XI–2. For example, we have seen that the proton occurs in the two configurations $u_\uparrow u_\uparrow d_\downarrow$ and $u_\uparrow u_\downarrow d_\uparrow$ with probabilities $2/3$ and $1/3$, respectively. This can be used to carry out the construction defined by Eq. (2.1) as follows:

$$\mu_p = \frac{2}{3} \mu(u_\uparrow u_\uparrow d_\downarrow) + \frac{1}{3} \mu(u_\uparrow u_\downarrow d_\uparrow)$$
$$= \frac{2}{3}[2\mu(u_\uparrow) + \mu(d_\downarrow)] + \frac{1}{3}[\mu(u_\downarrow) + \mu(u_\uparrow) + \mu(d_\uparrow)] = \frac{4}{3}\mu_u - \frac{1}{3}\mu_d, \tag{2.2}$$

and similarly for the other baryons. Experimental and quark model values are displayed in Table XII–2.

It is of interest to see how well the assumption of $SU(3)$ symmetry fares. In the limit of degenerate quark mass (denoted by a superbar), the quark magnetic moments are proportional to the quark electric charges,

$$\bar{\mu}_d = \bar{\mu}_s = -\frac{1}{2}\bar{\mu}_u \qquad (SU(3) \text{ limit}), \tag{2.3a}$$

---

[3] When referring to the 'magnetic moment' of a quantum system, one means the maximum component along a quantization axis (often chosen as the 3-axis). Thus, the magnetic moment is sensitive to the third component of quark spin as weighted by the quark magnetic moment.

Table XII–2. *Baryon magnetic moments.*

Mode	Experiment[a]	Quark model	Fit A[b]	Fit B[c]
μ_p	2.792847386(63)	$\frac{4\mu_u - \mu_d}{3}$	2.79	2.79
μ_n	$-1.91304275(45)$	$\frac{4\mu_d - \mu_u}{3}$	-1.86	-1.91
μ_Λ	$-0.613(4)$	μ_s	-0.93	-0.61
μ_{Σ^+}	2.458(10)	$\frac{4\mu_u - \mu_s}{3}$	2.79	2.67
$\lvert\mu_{\Sigma^0\Lambda}\rvert$	1.61(8)	$\frac{\lvert\mu_u - \mu_d\rvert}{\sqrt{3}}$	1.61	1.63
μ_{Σ^-}	$-1.160(25)$	$\frac{4\mu_d - \mu_s}{3}$	-0.93	-1.09
μ_{Ξ^0}	$-1.250(14)$	$\frac{4\mu_s - \mu_u}{3}$	-1.86	-1.44
μ_{Ξ^-}	$-0.651(3)$	$\frac{4\mu_s - \mu_d}{3}$	-0.93	-0.49

[a] Expressed in units of the nucleon magneton $\mu_N = e\hbar/2M_p$.
[b] $SU(3)$ symmetric fit.
[c] μ_u, μ_d, μ_s taken as independent parameters.

while isospin symmetry would imply

$$\bar{\mu}_d = -\frac{1}{2}\bar{\mu}_u \qquad (SU(2) \text{ limit}). \tag{2.3b}$$

If we determine the one free parameter by fitting to the very precisely known proton moment, we obtain the $SU(3)$ symmetric Fit A shown in Table XII–2. More generally, allowing μ_u, μ_d, μ_s to differ and determining them from the proton, neutron, and lambda moments yields

$$\mu_u = 1.85 \, \mu_N, \qquad \mu_d = -0.972 \, \mu_N, \qquad \mu_s = -0.613 \, \mu_N, \tag{2.4}$$

and leads to the improved (but not perfect) agreement of Fit B in Table XII–2. We see from Eq. (2.4) that the main effect of $SU(3)$ breaking is to substantially reduce the magnetic moment of the strange quark relative to that of the down quark. The deviation of μ_d/μ_u from the isospin expectation of $\mu_d/\mu_u = -1/2$ is smaller and perhaps not significant. Observe that the famous prediction of the $SU(2)$ limit, $\mu_n/\mu_p = -2/3$, is very nearly satisfied.

The magnetic moment as derived from the multipole expansion of the electric current is defined by

$$\boldsymbol{\mu} = \frac{1}{2}\int d^3x \, \mathbf{r} \times \mathbf{J}_{\text{em}}(x). \tag{2.5}$$

It follows from this expression that the contribution of a nonrelativistic quark 'q' to the hadronic magnetic moment is just the Dirac result,

$$\mu_q = \frac{Q}{2M_q}, \tag{2.6}$$

where M_q is the quark's constituent mass and Q is its charge. We can use this together with Eq. (2.4) to determine the constituent quark masses, with the result

$$M_u \simeq M_d \simeq 320 \text{ MeV}, \qquad M_s \simeq 510 \text{ MeV}. \tag{2.7}$$

As we shall see in Sect. XIII–1, these masses are comparable to those extracted from mass spectra of the light hadrons.

One can also construct models involving relativistic quarks. For these, the magnetic-moment contribution of an individual quark becomes

$$\boldsymbol{\mu} = \frac{2Q}{3}\boldsymbol{\sigma} \int d^3x \, r \, u(r) \, \ell(r). \tag{2.8}$$

Note the absence of an explicit dependence on quark mass. This is compensated by some appropriate dimensional quantity. The inverse radius R^{-1} plays this role in the bag model, and other determinations of R allow for a prediction of the hadronic magnetic moment. For example, the bag model defined by taking zero quark mass (corresponding to the ultrarelativistic limit) and $R = 1$ fm yields the value $\mu_p \simeq 2.5$ in a treatment which takes center-of-mass corrections into account [DoJ 80]. Although this specific value is somewhat too small, it is fair to say that quark models give a reasonable first approximation to baryon magnetic moments.

Semileptonic matrix elements

The most general form for the hadronic weak current in the transition $B_1 \to B_2 \ell \bar{\nu}_\ell$ is

$$\langle B_2(\mathbf{p}_2)|J_\mu^{(\text{wk})}|B_1(\mathbf{p}_1)\rangle$$
$$= \bar{u}(\mathbf{p}_2)\left[f_1(q^2)\gamma_\mu - \frac{i f_2(q^2)}{m_1 + m_2}\sigma_{\mu\nu}q^\nu + \frac{f_3(q^2)}{m_1 + m_2}q_\mu \right.$$
$$\left. + g_1(q^2)\gamma_\mu\gamma_5 - \frac{i g_2(q^2)}{m_1 + m_2}\sigma_{\mu\nu}q^\nu\gamma_5 + \frac{g_3(q^2)}{m_1 + m_2}q_\mu\gamma_5 \right]u(\mathbf{p}_1), \tag{2.9}$$

where the $\{f_i\}$ and $\{g_i\}$ form factors correspond respectively to the vector and axial-vector current matrix elements, and $q = p_1 - p_2$ is the momentum transfer.[4] The form factors are all functions of q^2 and the phases are chosen so that each form factor is real-valued if time-reversal invariance is respected. In practice, the form factors accompanying the two terms with the kinematical factor q_μ are difficult to observe because each such contribution is multiplied by a (small) lepton mass upon being contracted with a leptonic weak current. Thus, we shall drop these until Sect. XII–4.

---

[4] Given the context of application, there should be no confusion between the *QCD* strong coupling constant g_3 and the axial-vector form factor $g_3(q^2)$.

As regards the remaining form factors, we have already presented the ingredients for performing a quark model analysis (see also [DoGH 86b]). Using the $n \to p$ transition as a prototype, we have

$$f_1^{np} = \langle p_\uparrow | \int d^3x \ \bar{u}\gamma^0 d \ |n_\uparrow\rangle = \int d^3x \ (u_u u_d + \ell_u \ell_d) = 1 \ , \quad (2.10a)$$

$$\frac{f_1^{np} + f_2^{np}}{m_p + m_n} = \langle p_\uparrow | \int d^3x \ \frac{1}{2} [\mathbf{r} \times (\bar{u}\boldsymbol{\gamma} d)]_3 \ |n_\uparrow\rangle$$

$$= \frac{1}{3} \int d^3x \ r(u_u \ell_d + u_d \ell_u) = \frac{1}{2} \left(\frac{1}{2M_u} + \frac{1}{2M_d} \right) \ , \quad (2.10b)$$

$$g_1^{np} = \langle p_\uparrow | \int d^3x \ \bar{u}\gamma_3\gamma_5 d \ |n_\uparrow\rangle = \frac{5}{3} \int d^3x \ (u_u u_d - \frac{1}{3}\ell_u \ell_d), \quad (2.10c)$$

$$\frac{g_2^{np}}{m_n + m_p} + \left(\frac{1}{2m_n} - \frac{1}{2m_p} \right) \frac{g_1^{np} + g_3^{np}}{2} = \langle p_\uparrow | -i \int d^3x \ z\bar{u}\gamma^0\gamma_5 d \ |n_\uparrow\rangle$$

$$= \frac{1}{3} \int d^3x \ z(u_d \ell_u - u_u \ell_d) = \frac{1}{2} \left(\frac{1}{2M_d} - \frac{1}{2M_u} \right). \quad (2.10d)$$

In each case, we first give the defining relation, then the general Dirac wavefunction (cf. Eq. (1.4)) and, finally, the nonrelativistic quark model limit. The vanishing of g_2^{np} in the limit of exact isospin symmetry is a consequence of *G-parity* (cf. Sect. V–3)).

Predictions for the other baryonic transitions are governed by $SU(3)$ invariance, amended by small departures from $SU(3)$ invariance as suggested by the quark model, i.e., $s \to u$ transitions are similar to those of $d \to u$ as given above, but with the down-quark mass and wavefunction replaced by those of the strange quark. $SU(3)$ breaking in the form factors arises from this difference in the wavefunction. As a quark gets heavier, its wavefunction is more concentrated near the origin and the lower component becomes less important. The form factors of the matrix element $\langle B_b | J_c^\mu | B_a \rangle$ evaluated in the $SU(3)$ limit at $q^2 = 0$ give for the vector current,

$$f_1(0) = i f_{abc}, \qquad\qquad f_2(0) = i f_{abc} f + d_{abc} d,$$

$$f = \frac{1}{2}(\mu_p + \mu_n - 1), \qquad d = -\frac{3}{2}\mu_n, \qquad\qquad (2.11a)$$

with $f/d = 0.29$, and for the axial-vector current,

$$g_1(0) = i f_{abc} F + d_{abc} D, \qquad\qquad (2.11b)$$

with $F + D = g_1^{np} = g_A = 1.27$. In the above, the indices $a, b, c = 1, \dots, 8$ label the $SU(3)$ of flavor, with $c = (1 + i2)$ for $\Delta S = 0$ and $c = 4 + i5$ for $\Delta S = 1$. There is no $SU(3)$ parameterization for the g_2 form factor because it vanishes in the

$SU(3)$ limit. An important result specific to the quark model is $D/(D+F) = 3/5$ for the $SU(3)$ structure of the axial-current $\{g_1\}$ form factors.

$SU(3)$ breaking in the $\{f_1\}$ form factors is required by the Ademollo–Gatto theorem to occur only beginning at second order (see Sect. VIII–1). In practice, the quark model prediction for $SU(3)$ breaking yields an extremely small effect. This is not true for the $\{f_2\}$ form factors of weak magnetism, where inclusion of the strange-quark mass lowers all $s \to u$ transitions by 20% compared to the $d \to u$ transition. The wavefunction overlaps in g_1 lead to a slight increase in the strength of the $s \to u$ transition compared to $d \to u$ because of the reduced lower component of the s quark. For g_2, a nonzero but highly model-dependent value is generated, typically of order $|g_2/g_1| \simeq 0.3$.

XII–3 Symmetry properties and masses

In our discussion of baryon properties, we have first discussed quark models because they are generally simple and have predictive power. However, effective field theory methods are also useful when applied to the study of baryons.[5] We shall combine the two descriptions in this section.

Effective lagrangians for baryons

We begin by writing effective lagrangians which include *baryon* fields, using the procedure described in App. B–4. The lowest-order $SU(2)$-invariant lagrangian describing the nucleon and its pionic couplings has the form

$$\mathcal{L}_N = \bar{N} \left(i \slashed{\mathcal{D}} - g_A \overline{\slashed{A}} \gamma_5 - \mathbf{m}_0 \right) N$$
$$- \frac{Z_0}{2} \bar{N} \left(\xi \hat{\mathbf{m}} \xi + \xi^\dagger \hat{\mathbf{m}} \xi^\dagger \right) N - \frac{Z_1}{2} \bar{N} N \ \mathrm{Tr} \left(\hat{\mathbf{m}} U + U^\dagger \hat{\mathbf{m}} \right),$$
$$\mathcal{D}_\mu \equiv \partial_\mu + i \overline{V}_\mu, \qquad \xi \equiv \exp \left[i \boldsymbol{\tau} \cdot \boldsymbol{\pi} / (2 F_\pi) \right], \qquad U \equiv \xi \xi,$$
$$\overline{V}_\mu \equiv -\frac{i}{2} \left(\xi^\dagger \partial_\mu \xi + \xi \partial_\mu \xi^\dagger \right), \qquad \overline{A}_\mu \equiv -\frac{i}{2} \left(\xi^\dagger \partial_\mu \xi - \xi \partial_\mu \xi^\dagger \right), \qquad (3.1)$$

where $N = \binom{p}{n}$ is the nucleon field, $\hat{\mathbf{m}}$ is the mass matrix for current quarks (with $m_u = m_d \equiv \hat{m}$), Z_0 and Z_1 are arbitrary constants which parameterize terms proportional to the quark mass matrix, and the constant g_A is the nucleon axial-vector coupling constant $g_A \simeq 1.27$ (cf. Prob. XII–1). The mass parameter m_0 represents the nucleon mass in the $SU(2)$ chiral limit.

---

[5] There is also an effective field theory treatment of the few nucleon case [We 90, Va 08, EpM 12] which helps understand nuclei in a systematic manner.

For the full $SU(3)$ octet of baryons, the analog of 'N' is

$$B = \frac{1}{\sqrt{2}} \sum_{a=1}^{8} \lambda^a B^a = \begin{pmatrix} \frac{\Sigma^0}{\sqrt{2}} + \frac{\Lambda}{\sqrt{6}} & \Sigma^+ & p \\ \Sigma^- & -\frac{\Sigma^0}{\sqrt{2}} + \frac{\Lambda}{\sqrt{6}} & n \\ \Xi^- & \Xi^0 & -\frac{2\Lambda}{\sqrt{6}} \end{pmatrix}, \tag{3.2}$$

where the phases have been adjusted to match our quark model phase convention of Eq. (XI–1.8). The $SU(3)$ version of Eq. (3.1) becomes

$$\begin{aligned} \mathcal{L}_B = {}& \text{Tr}\left(\bar{B}\left(i\slashed{\mathcal{D}} - \bar{m}_0\right)B - D\left(\bar{B}\gamma^\mu\gamma_5\{\overline{A}_\mu, B\}\right) - F\left(\bar{B}\gamma^\mu\gamma_5[\overline{A}_\mu, B]\right)\right) \\ & - \frac{Z_0}{2}\,\text{Tr}\left(d_m\left(\bar{B}\{\xi\mathbf{m}\xi + \xi^\dagger\mathbf{m}\xi^\dagger, B\}\right) + f_m\left(\bar{B}\left[\xi\mathbf{m}\xi + \xi^\dagger\mathbf{m}\xi^\dagger, B\right]\right)\right) \\ & - \frac{Z_1}{2}\,\text{Tr}\left(\bar{B}B\right)\text{Tr}\left(\mathbf{m}U + U^\dagger\mathbf{m}\right), \end{aligned} \tag{3.3}$$

where the covariant derivative is now $\mathcal{D}_\mu B \equiv \partial_\mu B + i[\overline{V}_\mu, B]$, $\boldsymbol{\xi}$ is the $SU(3)$ generalization of the quantity in Eq. (3.1) with $\boldsymbol{\tau}$ replaced by $\boldsymbol{\lambda}$, $\mathbf{m}$ is the diagonal $SU(3)$ quark mass matrix,

$$\mathbf{m} = \left(\hat{m}, \hat{m}, m_s\right)_{\text{diag}} = \frac{1}{3}(2\hat{m} + m_s)\mathbf{1} + \frac{1}{\sqrt{3}}(\hat{m} - m_s)\lambda_8, \tag{3.4}$$

and $\bar{m}_0$ is the degenerate baryon mass in the $SU(3)$ chiral limit. Consistency of the $SU(2)$ and $SU(3)$ lagrangians requires

$$\begin{aligned} D + F &= g_\text{A}, \qquad d_m + f_m = 1, \\ m_0 &= \bar{m}_0 + Z_1 m_s - Z_0 m_s (f_m - d_m). \end{aligned} \tag{3.5}$$

The description thus far is based on symmetry. It includes quark mass, but not higher powers of derivatives.

Baryon mass splittings and quark masses

The various parameters ($\hat{m}, m_s, Z_0$ etc.) appearing in the chiral lagrangians of Eqs. (3.1), (3.3) can be determined from baryon mass and scattering data. In the nonstrange sector, the nucleon mass is given in the notation of Eq. (3.1) as

$$m_N = m_0 + (Z_0 + 2Z_1)\hat{m}. \tag{3.6}$$

To isolate the effect of the nonstrange quark mass $\hat{m}$ and of the constants Z_0, Z_1, it will prove useful to define a quantity σ,

$$\sigma = m_N - m_0 = \hat{m}\,\frac{\langle N|\bar{u}u + \bar{d}d|N\rangle}{2m_N} = \hat{m}\,(Z_0 + 2Z_1). \tag{3.7}$$

Shortly, we shall see how this quantity can be determined from pion–nucleon scattering data.

However, let us first consider the baryonic mass splittings generated by the mass difference $m_s - \hat{m}$. Upon using Eq. (3.3) to obtain expressions for the baryon masses and working with isospin-averaged masses, it is possible by adopting the numerical values

$$Z_0(m_s - \hat{m}) = 132\,\text{MeV}, \qquad d_m/f_m = -0.31, \qquad (3.8)$$

to obtain the following good fit:

$$
\begin{aligned}
m_\Sigma - m_N &= (f_m - d_m)Z_0(m_s - \hat{m}) = 251\,\text{MeV} \quad (\text{expt.} : 254.2\,\text{MeV}), \\
m_\Sigma - m_\Lambda &= -\frac{4}{3}d_m Z_0(m_s - \hat{m}) = 79\,\text{MeV} \qquad (\text{expt.} : 77.5\,\text{Mev}), \qquad (3.9) \\
m_\Xi - m_N &= 2f_m Z_0(m_s - \hat{m}) = 383\,\text{MeV} \qquad (\text{expt.} : 379.2\,\text{MeV}).
\end{aligned}
$$

Observe that these mass splittings depend on Z_0 but not on Z_1. The three relations of Eq. (3.9) imply the Gell-Mann–Okubo formula [Ge 61, Ok 62],

$$
\begin{aligned}
m_\Sigma - m_N &= \frac{1}{2}(m_\Xi - m_N) + \frac{3}{4}(m_\Sigma - m_\Lambda) \\
&(\text{Expt.} : 254\,\text{MeV} = 248\,\text{MeV}), \qquad (3.10)
\end{aligned}
$$

which displays an impressive level of agreement ($\simeq 3\%$) with experimental values.

The above analysis, based on a chiral lagrangian, can be enhanced by using ideas taken from the quark model. In the limit of *noninteracting* quarks, the quark model yields for a general spatial wavefunction,[6]

$$m_\Lambda - m_N = m_\Sigma - m_N = m_\Xi - m_\Sigma = (m_s - \hat{m})\int d^3x \, (u^2 - \ell^2). \qquad (3.11)$$

However, observe that $m_\Sigma = m_\Lambda$ (corresponding in the chiral lagrangian description to $d_m = 0$) for noninteracting quarks. Of course, the actual Λ and Σ baryons are not degenerate, so additional physics is required. A quark model source of the $\Lambda - \Sigma$ mass splitting lies in the hyperfine interaction of Eq. (XI–2.14),

$$H_{\text{hyp}}^{(\text{baryon})} = \frac{1}{2}\sum_{i<j}\bar{\mathcal{H}}_{ij}\mathbf{s}_i \cdot \mathbf{s}_j \, \delta^{(3)}(\mathbf{r}), \qquad (3.12)$$

where the prefactor of $1/2$ is associated with the color dependence of Eq. (XI–2.4). Matrix elements of this operator give rise to the additive mass contributions,

---

[6] One could equivalently use the language of the potential model, where these baryon mass splittings arise from the constituent quark mass difference $M_s - \hat{M}$.

$$m_N = \cdots - \frac{3}{8}\mathcal{H}_{\text{nn}}, \qquad\qquad m_\Lambda = \cdots - \frac{3}{8}\mathcal{H}_{\text{nn}},$$

$$m_\Sigma = \cdots + \frac{1}{8}\mathcal{H}_{\text{nn}} - \frac{1}{2}\mathcal{H}_{\text{ns}}, \quad m_\Xi = \cdots - \frac{1}{2}\mathcal{H}_{\text{ns}} + \frac{1}{8}\mathcal{H}_{\text{ss}}, \tag{3.13}$$

where $\bar{\mathcal{H}}_{ij}$ and $\mathcal{H}_{ij}$ are related by $\mathcal{H}_{ij} \equiv \bar{\mathcal{H}}_{ij}|\Psi(\mathbf{0})|^2$ and the subscripts 'n', 's' denote an interaction involving a nonstrange quark and a strange quark respectively. For $\mathcal{H}_{\text{nn}} \neq \mathcal{H}_{\text{ns}}$, the Σ and Λ will not be degenerate. Treating both quark mass splittings and hyperfine effects as first-order perturbations (e.g. $\mathcal{H}_{\text{ss}} - \mathcal{H}_{\text{ns}} = \mathcal{H}_{\text{ns}} - \mathcal{H}_{\text{nn}}$), one obtains quark model mass relations

$$m_\Lambda - m_N = (m_s - \hat{m})\int d^3x\,(u^2 - \ell^2),$$

$$m_\Sigma - m_\Lambda = \frac{1}{2}(\mathcal{H}_{\text{nn}} - \mathcal{H}_{\text{ns}}),$$

$$m_\Xi - m_N = \frac{1}{4}(\mathcal{H}_{\text{nn}} - \mathcal{H}_{\text{ns}}) + 2(m_s - \hat{m})\int d^3x\,(u^2 - \ell^2) \tag{3.14}$$

in accord with the sum rule of Eq. (3.10). These formulae can provide an estimate of quark mass. For the usual range of quark model wavefunctions (encompassing both bag and potential descriptions), the overlap integral has magnitude

$$\int d^3x\,(u^2 - \ell^2) \simeq \frac{1}{2} \to \frac{3}{4}. \tag{3.15}$$

To the extent that this estimate is valid, it produces the values

$$m_s - \hat{m} \simeq 230 \to 350\,\text{MeV}, \qquad \hat{m} \simeq 11 \to 14\,\text{MeV}, \tag{3.16}$$

where the chiral symmetry mass ratio of Eq. (VII–1.15a) has been used to obtain $\hat{m}$. In general, quoting absolute values of quark masses is dangerous as one must specify how the operator $\overline{q}q$, which occurs in the mass term $m_q\overline{q}q$, has been renormalized. It is all too common in the literature to ignore this point by using $m_s - \hat{m} = m_\Lambda - m_N$. The values quoted here are actually current-quark mass differences, renormalized at a hadronic scale using quark model matrix elements.

The parameter Z_1 which appears in the $SU(3)$ lagrangian of Eq. (3.3) is difficult to constrain in a quark model. For example, one might consider the matrix element

$$\frac{\langle N\,|m_s\overline{s}s|\,N\rangle}{2m_N} = m_s\,(Z_1 - Z_0(f_m - d_m)). \tag{3.17}$$

The most naive assumption, that $\langle N\,|m_s\overline{s}s|\,N\rangle$ vanishes, would imply $Z_1 = Z_0$ $(f_m - d_m) \simeq 1.9\,Z_0$. However, one may legitimately question whether such an assumption is reasonable. We shall return to the issue of the 'strangeness content' of the nucleon later in this section.

Goldberger–Treiman relation

Moving from the study of baryon masses to the topic of interactions, let us consider the coupling of pions and nucleons. The $SU(2)$ lagrangian of Eq. (3.1), expanded to order π^2, becomes

$$\mathcal{L}_N = \bar{N}(i\slashed{\partial} - m_N)N + \frac{g_A}{F_\pi}\bar{N}\gamma^\mu\gamma_5\frac{\boldsymbol{\tau}}{2}N \cdot \partial_\mu\boldsymbol{\pi}$$

$$- \frac{1}{4F_\pi^2}\bar{N}\gamma^\mu\boldsymbol{\tau}\cdot\boldsymbol{\pi}\times\partial_\mu\boldsymbol{\pi}\ N + \frac{1}{2F_\pi^2}\pi^2\bar{N}N\sigma + \cdots, \qquad (3.18)$$

where σ is defined in Eq. (3.7). The second term describes the $NN\pi$ vertex. Upon using Eq. (3.18) to compute the pion emission amplitude $N \to N\pi^i$ and comparing with the Lorentz invariant form

$$\mathcal{M}_{N\to N\pi^i} = -ig_{\pi NN}\bar{u}(\mathbf{p}')\gamma_5\tau^i u(\mathbf{p}), \qquad (3.19)$$

one immediately obtains the Goldberger–Treiman relation [GoT 58],

$$g_{\pi NN} = \frac{g_A m_N}{F_\pi}. \qquad (3.20)$$

Inserting the experimental value, $g_{\pi NN}^2/4\pi \simeq 13.8$, for the πNN coupling constant, one finds the Goldberger–Treiman relation to be satisfied to about 2.5%.

There also exist important implications for the g_3 term in the general expression given in Eq. (2.9) for the axial-current matrix element. In forming the $n \to p$ axial matrix element, one encounters a direct $\gamma_\mu\gamma_5$ contribution and also a pion-pole term which corresponds to pion propagation from the $n \to p\pi^-$ emission vertex to the axial current. Making use of Eq. (3.20) and Prob. XII–1, we have

$$\langle p(\mathbf{p}')|A_\mu^+|n(\mathbf{p})\rangle = \bar{u}(\mathbf{p}')\left[g_A\gamma_\mu\gamma_5 - \frac{g_A}{\sqrt{2}F_\pi}\slashed{q}\gamma_5\frac{\sqrt{2}F_\pi q_\mu}{q^2 - m_\pi^2}\right]u(\mathbf{p})$$

$$= \bar{u}(\mathbf{p}')\left[g_A\gamma_\mu\gamma_5 + \frac{2m_N g_A}{q^2 - m_\pi^2}q_\mu\gamma_5\right]u(\mathbf{p}). \qquad (3.21)$$

where $q = p - p'$. It is this induced pseudoscalar modification which allows the axial current to be conserved in the chiral limit $m_\pi^2 \to 0$,

$$-i\partial^\mu\langle p(\mathbf{p}')|A_\mu^+|n(\mathbf{p})\rangle = 2m_N g_A\left[1 - \frac{q^2}{q^2 - m_\pi^2}\right]\bar{u}(\mathbf{p}')\gamma_5 u(\mathbf{p})$$

$$= -\frac{2m_N g_A m_\pi^2}{q^2 - m_\pi^2}\bar{u}(\mathbf{p}')\gamma_5 u(\mathbf{p}). \qquad (3.22)$$

Note that for nonzero pion mass, the above is consistent with the PCAC relation of Eq. (B–3.7),

$$F_\pi m_\pi^2 \pi^k = \partial^\mu A_\mu^k, \qquad (3.23)$$

as both sides have the same matrix element,

$$-i\langle p(\mathbf{p}')\,|\,F_\pi m_\pi^2 \pi^+(0)\,|\,n(\mathbf{p})\rangle = i\sqrt{2}\,g_{\pi NN}\bar{u}(\mathbf{p}')\gamma_5 u(\mathbf{p})\frac{i}{q^2 - m_\pi^2}\sqrt{2}\,F_\pi m_\pi^2$$

$$= -\frac{2m_N g_A m_\pi^2}{q^2 - m_\pi^2}\bar{u}(\mathbf{p}')\gamma_5 u(\mathbf{p}). \qquad (3.24)$$

The pion-pole contribution of the axial-vector current-matrix element has been probed in nuclear muon capture, as will be described in Sect. XII–4.

The nucleon sigma term

One of the features immediately apparent from the effective lagrangian of Eq. (3.1) is that all the couplings of pions to nucleons, with the exception of the quark mass terms, are derivative couplings. Before turning to the sigma term, which appears in the nonderivative sector, let us briefly consider the expansion in powers of the number of derivatives for pion-nucleon scattering. Recall for pion–pion scattering (cf. Sect. VI–4), there were no large masses and the chiral expansion was expressed in terms of m_π^2 or E_π^2. However, correction terms in the chiral expansion for nucleons will enter at relatively low energies since a term like $2p \cdot q \simeq 2m_p E_\pi$ can get large quickly (it is linear in the energy and has a large coefficient, e.g., $E_\pi = 250$ MeV gives $2m_p E_\pi = (700\,\text{MeV})^2$). To combat this difficulty, additional (but still general) inputs such as analyticity and crossing symmetry are often invoked. Fortified with these theoretical constraints, one then matches intermediate-energy data to the low-energy chiral parameterizations. The low-energy chiral results thereby obtained appear to be well satisfied [Hö 83, GaSS 88].

The *nonderivative* pion–nucleon coupling coming from the quark mass terms in Eq. (3.1) is of particular interest. To determine this contribution from experiment, one must be able to suppress the various derivative couplings. Thus, if one extrapolated in the chiral limit to zero four-momentum, the derivative couplings would vanish. Not surprisingly then, a soft-pion analysis reveals that the nonderivative coupling can be isolated by extrapolating the isospin-even πN scattering amplitude with the Born term subtracted (called $\bar{D}^+$ in the literature) to the so-called 'Cheng–Dashen point' $t = m_\pi^2$, $s = m_N^2$ [ChD 71]. It is conventional to multiply the extrapolated amplitude by F_π^2 and thus define a quantity Σ,

$$\Sigma \equiv F_\pi^2\,\bar{D}_{CD}^+. \qquad (3.25)$$

To lowest order in the chiral expansion, the measured quantity Σ is just the matrix element σ defined in Eq. (3.7),

$$\Sigma = \sigma = \hat{m}\frac{\langle N|\bar{u}u + \bar{d}d|N\rangle}{2m_N}. \qquad (3.26)$$

It is this isospin-even scattering amplitude $\bar{D}^+$ which provides a unique window on the nonstrange quark mass $\hat{m}$. Because Σ is proportional to the small mass $\hat{m}$, it is difficult to determine this quantity precisely, and considerable effort has gone into its extraction. The Cheng–Dashen point lies outside the physical kinematic region, and extrapolation from the experimental region must be done carefully with dispersion relations. A recent estimate is [AlCO 13]

$$\Sigma = 59 \pm 7 \text{MeV}. \tag{3.27}$$

The result $\sigma = \Sigma - 15 \text{ MeV}$ has been obtained from studies of higher-order chiral corrections, implying

$$\sigma \simeq 44 \text{ MeV} \tag{3.28}$$

as the measure of light-quark mass [GaLS 91].

Strangeness in the nucleon

In light of the above discussion, it is tempting to interpret various contributions to the nucleon mass by making use of the energy-momentum trace. Recall the trace anomaly of Eq. (III–4.16),

$$\theta^\mu_\mu = \frac{\beta_{QCD}}{2g_3} F^a_{\mu\nu} F^{a\mu\nu} + m_u \bar{u}u + m_d \bar{d}d + m_s \bar{s}s. \tag{3.29}$$

Taking the nucleon matrix element gives

$$m_N = \frac{\langle N | \theta^\mu_\mu | N \rangle}{2m_N} = m_0 + \sigma,$$

$$m_0 = (2m_N)^{-1} \langle N \left| \frac{\beta_{QCD}}{2g_3} F^a_{\mu\nu} F^{a\mu\nu} + m_s \bar{s}s \right| N \rangle \simeq 894 \pm 8 \text{ MeV},$$

$$\sigma = \hat{m} \frac{\langle N | \bar{u}u + \bar{d}d | N \rangle}{2m_N} \simeq 44 \text{ MeV}. \tag{3.30}$$

This result is already quite interesting in that the largest contributions, the gluon and strange-quark terms in m_0, appear to be 'nonvalence'. At this stage, the separation is essentially model-independent.

One can explore the 'strangeness content of the nucleon' by using an $SU(3)$ analysis of hyperon masses. Thus, we introduce a mass-splitting operator, which transforms as the eighth component of an octet,

$$\mathcal{L}_{\text{m-s}} = \frac{1}{3}(\hat{m} - m_s)(\bar{u}u + \bar{d}d - 2\bar{s}s). \tag{3.31}$$

Since the hyperon mass splittings are governed by this octet operator, we find

$$\delta_s \equiv \frac{\langle p \left|(m_s - \hat{m})(\overline{u}u + \overline{d}d - 2\overline{s}s)\right| p \rangle}{2m_p} = \frac{3}{2}(m_\Xi - m_N) = 574\,\text{MeV}. \quad (3.32a)$$

When scaled by the quark mass ratio $\hat{m}/m_s$, Eq. (3.32a) becomes

$$\delta \equiv \hat{m} \frac{\langle N \left|\overline{u}u + \overline{d}d - 2\overline{s}s\right| N \rangle}{2m_N}$$

$$= \frac{3}{2} \frac{m_\pi^2}{m_K^2 - m_\pi^2}(m_\Xi - m_\Lambda) \simeq 25\,\text{MeV} \quad (35\,\text{MeV}), \quad (3.32b)$$

where the figure in parentheses includes higher-order chiral corrections [Ga 87]. Comparison of δ and σ immediately indicates that they are compatible only if the strange-quark matrix element does *not* vanish. Indeed, one requires

$$\frac{\langle N \left|\overline{s}s\right| N \rangle}{\langle N \left|\overline{u}u + \overline{d}d + \overline{s}s\right| N \rangle} \simeq 0.18 \quad (0.09). \quad (3.33)$$

This gives for the constant Z_1 of Eq. (3.1) the value $Z_1 \simeq 3.9 Z_0$ (2.9 Z_0) to be contrasted with the estimate which follows Eq. (3.17). At the same time, one can separate out the following matrix elements

$$(2m_N)^{-1}\langle N \left|\frac{\beta_{QCD}}{2g_3} F_{\mu\nu}^a F^{a\mu\nu}\right| N \rangle \simeq 634\,\text{MeV} \quad (764\,\text{MeV}),$$

$$(2m_N)^{-1}\langle N \left|m_s\overline{s}s\right| N \rangle \simeq 260\,\text{MeV} \quad (130\,\text{MeV}), \quad (3.34)$$

where figures in brackets use the corresponding bracketed quantity in Eq. (3.32b). Note the surprisingly large effect of the strange quarks. These results are controversial because they draw a counter-intuitive conclusion from the use of $SU(3)$ symmetry. However, even with $SU(3)$ breaking, the difference between σ and the $SU(3)$ value of δ is large enough that some $\overline{s}s$ contribution is likely to be required.

This analysis does not go well with the naive interpretation of the quark model as embodied, for example, in the proton-state vector formula which began this chapter. However, it is possibly compatible with a more sophisticated interpretation of the constituent quarks which enter into quark models. In the process of forming a constituent quark, the quark is 'dressed' by gluonic and even $\overline{s}s$ quark fields. It is no longer the naive object that occurs in the *QCD* lagrangian. It is this dressed object which may then easily generate gluonic and perhaps strange quark matrix elements. Recall that even the vacuum state has gluonic and quark matrix elements. Similar explanations exist in bag and Skyrme models [DoN 86]. This issue remains unresolved at present.

Based on the possible existence of a substantial nonzero value for the scalar density matrix element $\langle N|\overline{s}s|N\rangle$, a major program was launched to investigate

the possibility for a similar nonzero value for the strange vector-current matrix element $\langle N|\bar{s}\gamma_\mu s|N\rangle$ which can be characterized in terms of charge and magnetic form factors $F_1^s(q^2)$, $F_2^s(q^2)$ via

$$\langle N|\bar{s}\gamma_\mu s|N\rangle = \bar{u}(p')\left[\gamma_\mu F_1^s(q^2) - \frac{i}{2m_N}\sigma_{\mu\nu}q^\nu F_2^s(q^2)\right]u(p). \qquad (3.35)$$

The form factor $F_1^s(q^2)$ obeys $F_1^s(0) = 0$, whereas $F_2^s(q^2)$ has no such constraint.[7] In order to determine the size of the $\bar{u}\gamma_\mu u$, $\bar{d}\gamma_\mu d$, $\bar{s}\gamma_\mu s$ contributions to the corresponding nucleon matrix elements, three experimental inputs are required. Two of these come from well-known electromagnetic form factors of the proton and neutron. The third can be found by performing parity-violating electron-scattering experiments from the proton, by measuring the difference in the cross sections for the scattering of electrons with left- and right-handed helicities. This is sensitive to the strange-quark current because the electromagnetic current and the neutral weak current involve strange quarks with different strengths. In this case there exists an interference between the electromagnetic (γ-exchange) and weak (Z^0-exchange) contributions and the resultant asymmetry will have the form

$$A_{LR} = \frac{d\sigma_R - d\sigma_L}{d\sigma_R + d\sigma_l} \sim \frac{Gq^2}{4\pi\sqrt{2}\alpha}\left(M_E + M_M + \cdots\right), \qquad (3.36)$$

where M_E, M_M involve the interference of the electromagnetic and electric, magnetic weak form factors and the ellipses indicate a small piece involving the vector electron coupling and the axial current. In this asymmetry, the electron side involves an axial current while the nucleon side involves a vector current. This asymmetry has been studied as a function of q^2 in a series of experiments at electron laboratories at MIT-Bates, at Jefferson Laboratory, and at the Mainz microtron. The result is that no signal for a strange vector-current matrix element has been seen and limits have been placed on the strange form factors. Numerically, strange quarks contribute less than 5% of the mean square charge radius and less than 10% of the magnetic moment of the proton. Reviews of this body of work can be found in [ArM 12] and [BeH 01].

Quarks and nucleon spin structure

The constituent quark model provides a simple picture of the contents of baryons as systems composed of three constituent quarks and nothing else. A rigorous description using the quark and gluon degrees of freedom which appear in the fundamental

---

[7] The condition on $F_1^s(0)$ is a consequence of current conservation. Equivalently, taking $\mu = 0$ in Eq. (3.35) and integrating over the proton volume, one encounters the strangeness 'charge' $S \equiv \int d^3x\, s^\dagger(\mathbf{x})s(\mathbf{x})$ and $S|N\rangle = 0$ since the nucleon carries no net strangeness.

lagrangian is in general more complex, but it is often nevertheless instructive to explore the constituent picture of a given observable. An interesting example is the spin structure of the nucleon.

For any Lorentz invariant theory, Noether's theorem requires that there exist an angular momentum tensor $M^{\mu\alpha\beta}$ which is conserved ($\partial_\mu M^{\mu\alpha\beta} = 0$) and which gives rise to three angular momentum charges associated with rotational invariance,

$$J^{\alpha\beta} \equiv \int d^3x \, M^{0\alpha\beta}(x). \tag{3.37}$$

In the rest frame of a particle, the $\{J^{\alpha\beta}\}$ are related to the three components of angular momenta via

$$J^i = \frac{1}{2}\epsilon^{ijk} J^{jk}. \tag{3.38}$$

For the example of a free fermion, the above quantities take the form

$$M^{\mu\alpha\beta} = i\bar{\psi}\gamma^\mu \left(x^\alpha \partial^\beta - x^\beta \partial^\alpha\right)\psi + \frac{1}{2}\bar{\psi}\gamma^\mu \sigma^{\alpha\beta}\psi, \tag{3.39}$$

up to total derivatives which do not contribute to the charges, and

$$\mathbf{J} = \int d^3x \left[-i\psi^\dagger (\mathbf{x} \times \boldsymbol{\partial})\psi + \frac{1}{2}\bar{\psi}\boldsymbol{\gamma}\gamma_5\psi\right] \equiv \mathbf{L} + \mathbf{S}. \tag{3.40}$$

The two contributions in Eq. (3.40) may be labeled the orbital and spin components of the angular momentum.

The quarks in the Noether current are lagrangian (current) quarks, not constituent quarks. Nevertheless, in the spirit of the quark model let us apply Eq. (3.40) to the quarks in a spin-up proton. As expressed in terms of upper (u) and lower (ℓ) components (cf. Eq. (XI–1.13)), the orbital and spin contributions are found to be

$$\langle \mathbf{L} \rangle = \frac{2}{3}\int d^3x \, \ell^2 \langle\boldsymbol{\sigma}\rangle, \qquad \langle \mathbf{S} \rangle = \int d^3x \left(u^2 - \frac{1}{3}\ell^2\right)\frac{\langle\boldsymbol{\sigma}\rangle}{2}. \tag{3.41}$$

Aside from the factor $1/2$ occurring in $\boldsymbol{\sigma}/2$, the quark spin contribution to $\mathbf{S}$ is just the axial-vector matrix element of Eq. (1.24), whereas the orbital angular momentum contains just the lower component ℓ because the $\mathbf{x} \times \boldsymbol{\partial}$ operator has a nonzero effect only when acting on the $\boldsymbol{\sigma} \cdot \hat{\mathbf{x}}$ factor in the lower component of Eq. (XI–1.13). Observe that the orbital angular momentum is nonvanishing and proportional to the quark spin. The spin and orbital portions for the individual u, d flavors are easily computed to yield

$$\langle S_z^{(u)} \rangle = \frac{2}{3}\int d^3x \left(u^2 - \frac{1}{3}\ell^2\right), \qquad \langle S_z^{(d)} \rangle = -\frac{1}{6}\int d^3x \left(u^2 - \frac{1}{3}\ell^2\right),$$

$$\langle L_z^{(u)} \rangle = \frac{8}{9}\int d^3x \, \ell^2, \qquad\qquad \langle L_z^{(d)} \rangle = -\frac{2}{9}\int d^3x \, \ell^2. \tag{3.42}$$

A first lesson is that, despite the spin wavefunction of the protons being written entirely in terms of quarks as in Table XI–2, the quark spin averages of Eq. (3.42) do *not* add up to yield the proton spin. The sum is reduced from the anticipated value of $1/2$ by the lower component ℓ in the Dirac spinor. It is the total angular momentum $\mathbf{J}$ which has the expected result,

$$\langle \mathbf{J} \rangle = \frac{1}{2} \langle \boldsymbol{\sigma} \rangle, \tag{3.43}$$

but the total is split up between the orbital and spin components. The bag model, for example, yields

$$\langle \mathbf{S} \rangle \simeq 0.65 \, \langle \mathbf{J} \rangle, \tag{3.44}$$

so about 35% of the nucleon spin arises from orbital angular momentum.

Of course, *QCD* is a full interacting theory and the discussion of the angular momenta of the quarks and the gluons cannot be fully separated because these fields interact with each other. The total angular momentum can be decomposed into several terms, including the interactions between the fields [JaM 90]. These can be grouped in various ways. In the current quark–gluon description, it is common to write

$$\frac{1}{2} = \frac{1}{2} S_q + L_q + J_g, \tag{3.45}$$

where S_q, L_q are the spin and angular momentum components carried by the quarks and J_g is that carried by the gluons. Thus, we have

$$\mathbf{J_q} = \int d^3 x \left[\psi^\dagger \frac{\boldsymbol{\Sigma}}{2} \psi + \psi^\dagger \, \mathbf{x} \times (-\mathbf{iD}) \psi \right],$$

$$\mathbf{J_g} = \int d^3 x \, \mathbf{x} \times (\mathbf{E} \times \mathbf{B}), \tag{3.46}$$

where $\boldsymbol{\Sigma}$ is the usual Dirac spin matrix and $D_\mu \psi = [\partial_\mu + i g A_\mu] \psi$ is the covariant derivative of ψ and therefore, in this definition, the quark angular momentum has a gluonic component [JiTH 96].

Polarized deep-inelastic electron scattering from the nucleon can measure spin effects of the quarks. The study of spin dependent deep inelastic scattering involves the antisymmetric component of the nucleon tensor,[8] which can be written in the form

$$W^{[\mu\nu]} = \frac{1}{4\pi} \int d^4 x \, e^{-q \cdot x} \langle p, s | [J_\mu^{\text{em}}(x), J_\nu^{\text{em}}(0)] | p, s \rangle$$

$$= -i \epsilon_{\mu\nu\alpha\beta} q^\alpha \left[G_1(\nu, Q^2) \cdot \frac{s^\beta}{m_N^2} + G_2(\nu, Q^2) \cdot \frac{m_N \nu s^\beta - s \cdot q p^\beta}{m_N^4} \right], \tag{3.47}$$

---

[8] More details can be found in the review [Ba 05].

where $\nu = p \cdot q/m_N$ and $Q^2 = -q^2$. The scaling behavior of the two structure functions is

$$g_1(x, Q^2) = \frac{\nu}{m_N}G_1(\nu, Q^2), \qquad g_2(x, Q^2) = \left(\frac{\nu}{m_N}\right)^2 G_2(\nu, Q^2), \qquad (3.48)$$

where $x = Q^2/2m_N\nu$ is the Bjorken scaling variable. In the parton model, neglecting *QCD* renormalization, one determines

$$\int_0^1 dx\, g_1^p(x, Q^2) = \frac{1}{2}\sum_q e_q^2 \Delta q = \frac{1}{12}g_A^{(3)} + \frac{1}{36}g_A^{(8)} + \frac{1}{9}g_A^{(0)}, \qquad (3.49)$$

where $g_A^{(3)}$, $g_A^{(8)}$, $g_A^{(0)}$ are the isovector, $SU(3)$ octet, and flavor-singlet axial charges respectively. The axial charges are written in terms of their quark spin content as

$$2m_N s_\mu \Delta q = \langle p, s|\bar{q}\gamma_\mu\gamma_5 q|p, s\rangle, \qquad (3.50)$$

with

$$\Delta q = \int_0^1 dx\, (q_\uparrow(x) - q_\downarrow(x)), \qquad (3.51)$$

where $q_s(x)$ is the parton distribution function carrying spin s. In terms of the light quarks we have then

$$g_A^{(3)} = \Delta u - \Delta d, \quad g_A^{(8)} = \Delta u + \Delta d - 2\Delta s, \quad g_A^{(0)} = \Delta u + \Delta d + \Delta s. \quad (3.52)$$

The first two of these are well defined from the study of hyperon beta decay,

$$g_A^{(3)} = F + D = 1.27 \pm 0.003 \qquad \text{(from neutron beta decay)},$$
$$g_A^{(8)} = 3F - D = 0.58 \pm 0.03 \qquad \text{(from semileptonic hyperon decay)}. \quad (3.53)$$

The first of these is directly measured and the second comes from an $SU(3)$ rotation from the values that are obtained in an $SU(3)$ fit to $\Delta S = 1$ hyperon decay. Such a partonic analysis leads to a decomposition, $\Delta u = 0.84 \pm 0.01 \pm 0.02$, $\Delta d = -0.43 \pm 0.01 \pm 0.02$ and $\Delta s = -0.08 \pm 0.01 \pm 0.02$, where these numbers are from recent COMPASS data [Qu 12]. The sum of these, $\Delta u + \Delta d + \Delta s \sim 0.33$, is about half of what would be expected for the nucleon spin in the naive quark model, Eq. (3.44), and of course the quark model predicts that the Δs should be zero.

However, there is reason for caution in this interpretation. The singlet axial current,

$$J_\mu^0 = \bar{u}\gamma_\mu\gamma_5 u + \bar{d}\gamma_\mu\gamma_5 d + \bar{s}\gamma_\mu\gamma_5 s, \qquad (3.54)$$

whose matrix element is said to be represented by $\Delta u + \Delta d + \Delta s$, is anomalous, as seen in Sect. III–3. This has important consequences [AlR 88, Sh 08]. While

the axial currents which transform as $SU(3)$ octets have only finite multiplicative renormalization, the singlet current mixes with gluonic fields under radiative corrections. Different renormalization schemes yield different mixtures of the quark and gluon components [Sh 08]. Moreover, the quark component is not scale-independent; there is renormalization group running as a function of Q^2. Note that the other currents do not suffer from these problems. In particular, the Bjorken sum rule [Bj 66] involves the difference of the proton and neutron matrix elements, which then cancels out the isosinglet contributions, such that the first moment is independent of Q^2,

$$\int_0^1 dx \, g_1^{p-n}(x, Q^2) = \frac{1}{6} g_A^{(3)}. \tag{3.55}$$

This sum rule yields a value $g_A^{(3)} = 1.28 \pm 0.07 \pm 0.01$, which agrees well with the number $g_A^{(3)} = 1.270 \pm 0.003$ measured in neutron beta decay. The anomaly in the singlet current complicates the discussion of the quark contribution to the proton spin.

The partonic analysis of the quark spins has led to further studies. Attempts at the experimental study of the gluonic contributions has revealed only a small contribution to the nucleon spin [AiBHM 13]. There may be the possibility of studying the angular-momentum components through the concept of generalized parton distributions [Ji 94]. However, the experimental determination of these generalized parton distributions is yet to be achieved.

XII–4 Nuclear weak processes

One area in which the structure of the weak hadronic current has received a great deal of attention is that of nuclear beta decay and muon capture. Although in some sense this represents simply a nuclear modification of the basic weak transitions $n \rightarrow p + e^- + \bar{\nu}_e$, $p \rightarrow n + e^+ + \nu_e$, the use of nuclei allows specific features to be accented by the choice of levels possessing particular spins and/or parities [Ho 89]. Here, we shall confine our attention to *allowed* decays ($\Delta J = 0, \pm 1$, no parity change) and will emphasize those aspects which stress the structure of the weak current rather than that of the nucleus itself. In particular, nuclear beta decay provides the best determination of V_{ud}, while muon capture provides the only measurement of the pseudoscalar axial weak form factor predicted by chiral symmetry.

Measurement of V_{ud}

There are many occurrences in nuclei of an isotriplet of $J^P = 0^+$ states. Examples are found with $A = 10, 14, 26, 34, 42, \ldots$. Because Coulombic effects raise

the mass of the proton-rich $I_3 = 1$ state with respect to that with $I_3 = 0$, the positron emission process $N_1(I_z = 1) \rightarrow N_2(I_z = 0) + e^+ + \nu_e$ can occur. These transitions are particularly clean theoretically, and this is the reason why they are important. Since the transition is $0^+ \rightarrow 0^+$, only the vector current is involved, and because of the lack of spin there can be no weak magnetic form factor. The vector-current matrix element involves but a single form factor $a(q^2)$,

$$\langle N_2(p_2) | V_\mu | N_1(p_1) \rangle = a(q^2)(p_1 + p_2)_\mu. \tag{4.1}$$

This form factor is known at $q^2 = 0$ because the charged vector weak current V_μ is just the isospin rotation of the electromagnetic current,

$$[I_-, J_{\text{em}}^\mu] = \bar{d}\gamma^\mu u. \tag{4.2}$$

This relation is often called the *conserved vector current hypothesis* or CVC, and requires for each of the $0^+ \rightarrow 0^+$ transitions,

$$a(0) = \sqrt{2}. \tag{4.3}$$

What is generally quoted for such decays is the $\mathcal{F}t_{1/2}$ *value*, essentially the half-life $t_{1/2}$ multiplied by the (kinematic) phase space factor f plus various radiative and Coulomb corrections [WiM 72]. Theoretically, one expects a universal form

$$\mathcal{F}t_{1/2} = \frac{2\pi^3 \ln 2}{G_\mu^2 m_e^5 |V_{\text{ud}}|^2 a^2(0)} \left(1 - \frac{\alpha}{2\pi} (4 \ln(M_Z/m_N) + \cdots) \right), \tag{4.4}$$

which should be identical for each isotriplet transition. G_μ is the weak decay constant measured in muon decay while the logarithmic correction arises from 'hard'-photon corrections, as discussed in Chap. VII. The 'soft'-photon piece as well as finite-size and Coulombic corrections are contained in the phase space factor $\mathcal{F}$. Much careful experimental and theoretical study has been given to this problem, and the current situation is summarized in Table XII–3 where the experimental $\mathcal{F}t_{1/2}$ values are tabulated. A fit to these and additional Fermi decays produces the value $\mathcal{F}t_{1/2} = 3072.08 \pm 0.79$ s with chi-squared per degree of freedom $\chi^2/\nu = 0.28$. This excellent agreement over a wide range of Z values is evidence that soft-photon corrections are under control.

Comparison of the experimental $\mathcal{F}t_{1/2}$ value with the theoretical expression given in Eq. (4.4) yields the determination

$$V_{\text{ud}} = 0.97425(22), \tag{4.5}$$

which makes V_{ud} the most precisely measured component of the CKM matrix.

Table XII–3. *Energy release and* $\mathcal{F}t_{1/2}$ *values for*
$0^+ \rightarrow 0^+$ *Fermi decays [HaT 09].*

Nucleus	E_0(KeV)	$\mathcal{F}t_{1/2}$ (s)
^{10}C	885.87(11)	3076.7(4.6)
^{14}O	1809.24(23)	3071.5(3.3)
^{26m}Al	3210.66(06)	3072.4(1.4)
^{34}Cl	4469.64(23)	3070.2(2.1)
^{38m}K	5022.40(11)	3072.5(2.4)
^{42}Sc	5404.28(30)	3072.4(2.7)
^{46}V	6030.49(16)	3073.3(2.7)
^{50}Mn	6612.45(07)	3070.9(2.8)
^{54}Co	7222.37(28)	3069.9(3.2)

The pseudoscalar axial form factor

Chiral symmetry predicts a rather striking result for the form factor $g_3(q^2)$ of Eq. (2.9), namely that it is determined by the pion pole with a coupling fixed by the PCAC condition. One cannot detect this term in either neutron or nuclear beta decay because when the full matrix element is taken, one obtains

$$\frac{g_3}{2m_N}\overline{v}(\mathbf{p}_v)q_\mu\gamma^\mu(1+\gamma_5)u(\mathbf{p}_e) = \frac{g_3 m_e}{2m_N}\overline{v}(\mathbf{p}_v)(1-\gamma_5)u(\mathbf{p}_e), \qquad (4.6)$$

which is proportional to the electron mass and is thus too small to be seen (effects in the spectra are $\mathcal{O}(m_e^2/m_N E_e) \ll 1$). However, in the muon capture process $\mu^- p \rightarrow v_\mu n$, the corresponding effect is $\mathcal{O}(m_\mu/m_N) \sim 10\%$. Thus, muon capture is a feasible arena in which to study the chiral symmetry prediction [CzM 07]. The drawback in this case is that typically one has available from experiment only a *single* number, the capture rate. In order to interpret such experiments, one needs to know the value of each nuclear form factor at $q^2 \simeq -0.9\ m_\mu^2$, which introduces some uncertainty since these quantities are determined in beta decay only at $q^2 \simeq 0$. Nevertheless, predicted and experimental capture rates are generally in good agreement provided one assumes (i) the $q^2 \simeq 0$ value of form factors from the analogous beta decay, (ii) q^2 dependence of form factors from CVC and electron scattering results, (iii) the CVC value for the weak magnetic term f_2, and (iv) the PCAC value of Eq. (3.21) for g_3. The results are summarized in Table XII–4. Obviously, agreement is good except for ^{6}Li, for which the origin of the discrepancy is unknown, although it has been speculated that perhaps the spin mixture is not statistical. Also, in the case of ^{3}He there remains a small disagreement between the elementary particle model (EPM) and impulse approximation (IA) predictions for the capture rate.

Table XII–4. *Muon capture rates.*

Reaction	Theory (10^3 s^{-1})	Experiment (10^3 s^{-1})
$\mu^- + p \to \nu_\mu + n$	0.712 ± 0.005^a	$0.715 \pm 0.005 \pm 0.005^a$
$\mu^- + {}^3\text{He} \to \nu_\mu + {}^3\text{H}$	$1.537 \pm 0.022^{\text{EPM}}$ $1.506 \pm 0.015^{\text{IA}}$	1.496 ± 0.004
$\mu^- + {}^6\text{Li} \to \nu_\mu + {}^6\text{He}$	0.98 ± 0.15	$1.60^{+0.33}_{-0.12}$
$\mu^- + {}^{12}\text{C} \to \nu_\mu + {}^{12}\text{B}$	7.01 ± 0.16	$6.75^{+0.3}_{-0.75}$

$^a S_{\mu^- p} = 0$.

Before proceeding, we should emphasize one relevant point. When PCAC is applied, it is for the nucleon

$$2m_N g_1(q^2) - \frac{q^2}{2m_N} g_3(q^2) = 2F_\pi g_{\pi NN}(q^2) \left(1 - \frac{q^2}{m_\pi^2}\right)^{-1}. \qquad (4.7)$$

Then, at $q^2 = 0$, we have

$$1.27 = g_1(0) \simeq \frac{F_\pi g_{\pi NN}(m_\pi^2)}{m_N} = 1.30, \qquad (4.8)$$

which is the Goldberger–Treiman relation. On the other hand, taking similar q^2 dependence for $g_1(q^2)$ and $g_{\pi NN}(q^2)$, we find

$$\frac{m_\mu}{2m_N} \frac{g_3(-0.9m_\mu^2)}{g_1(-0.9m_\mu^2)} = \frac{2m_N m_\mu}{m_\pi^2 + 0.9m_\mu^2} - \frac{1}{3} r_A^2 m_\mu m_N \simeq 6.45. \qquad (4.9)$$

PCAC is generally applied in nuclei in the context of a simple impulse approximation, and it is this version of PCAC which is tested by the muon capture rates listed in Table XII–4. The direct application of PCAC in nuclei cannot generally be utilized since the pion couplings are unknown.

In the case of muon capture on ${}^{12}\text{C}$, additional experimental data are available. One class of experiment involves measurement of the polarization of the recoiling ${}^{12}\text{B}$ nucleus. Combining this measurement with that of the total capture rate yields a separate test of CVC as well as of PCAC. The results,

$$\frac{f_2^{\text{expt}}}{f_2^{CVC}} = 1.00 \pm 0.05, \qquad \frac{m_\mu}{2m_N} \frac{g_3(-0.9m_\mu^2)}{g_1(-0.9m_\mu^2)} = 8.0 \pm 3.0, \qquad (4.10)$$

are in good agreement with both symmetry assumptions.

In addition, one can measure the average and longitudinal recoil polarizations in the ^{12}C muon capture, yielding a value for the induced pseudoscalar coupling,

$$\frac{m_\mu}{2m_N} \frac{g_3(-0.9m_\mu^2)}{g_1(-0.9m_\mu^2)} = 9.0 \pm 1.7, \tag{4.11}$$

which is again in good agreement with PCAC.

The most precise value comes from the recent measurement of the singlet-muon capture rate in hydrogen, which yields

$$\frac{m_\mu}{2m_N} \frac{g_3(-0.9m_\mu^2)}{g_1(-0.9m_\mu^2)} = 5.75 \pm 0.95, \tag{4.12}$$

which is excellent agreement with PCAC.

XII–5 Hyperon semileptonic decay

The goals in studying hyperon semileptonic processes are to confirm the value of V_{us} obtained in kaon decay and to use the form factors to better understand hadronic structure. These two goals are interconnected. In earlier days when data were not very precise, fits to hyperon decays were made under the assumption of perfect $SU(3)$ invariance in order to extract V_{us}. Presently, the experiments are precise enough that exact $SU(3)$ no longer provides an acceptable fit. The desire to learn about V_{us} is thus impacted by the need to understand the $SU(3)$ breaking.

We have already described in Sect. XII–1 the physics ingredients which lead to $SU(3)$ breaking within a simple quark description. These include recoil or center-of-mass corrections, wavefunction mismatch (in which a normalization condition realized in the symmetry limit no longer holds), and generation of the axial form factor g_2. For hyperons, because of the presence of the axial current, $SU(3)$ breaking can occur in first order. This means that hyperon decays are more difficult to use for determining V_{us} than are kaon decays, where the Ademollo–Gatto theorem reduces the amount of symmetry breaking. Thus, at the moment it is probably best to use the value of V_{us} determined from kaon decay, and require that hyperon decays yield a consistent value.

The clearest evidence on $SU(3)$ breaking comes from the $\Sigma^- \to \Lambda + e^- + \bar{\nu}_e$ rate. Since this is a $\Delta S = 0$ process, V_{us} does not enter and, in addition, the vector current matrix element must vanish. Thus, the rate is determined by the axial-current contribution alone, for which the theoretical prediction is

$$g_1^{\Sigma^-\Lambda} = \rho\sqrt{\frac{2}{3}}\frac{D}{D+F}g_1^{np}, \tag{5.1}$$

where ρ is a $SU(3)$ breaking factor due to the center-of-mass effect. A bag-model estimate yields $\rho = 0.939$. Taking $\rho = 1$, the best $SU(3)$ symmetric fit to all the data [CaSW 03] would require $D/(D + F) = 0.635 \pm 0.006$, and hence $g_1^{\Sigma^- \Lambda} = 0.658$ if $SU(3)$ were exact. On the other hand, the data on $\Sigma^- \to \Lambda e \bar{\nu}_e$ requires $g_1^{\Sigma^- \Lambda} = 0.591 \pm 0.014$, which implies the correction $\rho = 0.931 \pm 0.022$. There seems to be no way to avoid this need for $SU(3)$ breaking.

The full pattern of $SU(3)$ breaking is more difficult to uncover. One problem is experimental. When the g_1 values are extracted from the data, they have generally been analyzed under the assumptions that the f_1 and f_2 form factors have exactly their $SU(3)$ values and that $g_2 = 0$. If these assumptions are not correct, then the values cited in [RPP 12] do not reflect the true g_1 but rather some combination of g_1, f_1, f_2, and g_2. The correlation with g_2 is particularly strong. Thus, quoted values of g_1 must be treated with caution.

The present status of these decays is reviewed in [CaSW 03]. The data can be fit well either by the center-of-mass correction described above, with $g_2 = 0$, or by the full corrections including wavefunction mismatch, with $g_2/g_1 = 0.20 \pm 0.07$ in $\Lambda \to p + e + \bar{\nu}_e$. Without an independent measurement of g_2 one cannot decide between these. We note, however, that either option yields a value of V_{us} consistent with that found in kaon decays,

$$V_{\mathrm{us}} = 0.2250 \pm 0.0027. \tag{5.2}$$

XII–6 Nonleptonic decay

The dominant decays of hyperons are the nonleptonic $B \to B'\pi$ modes. Because of the spin of the baryons and the many decay modes available, the nonleptonic hyperon decays present a richer opportunity for study than do the nonleptonic kaon decays.

Phenomenology

The $B \to B'\pi$ matrix elements can be written in the form

$$\mathcal{M}_{B \to B'\pi} = \bar{u}(\mathbf{p}')\left[A + B\gamma_5\right]u(\mathbf{p}), \tag{6.1}$$

with parity-violating (A) and parity-conserving (B) amplitudes. Watson's theorem implies that if CP is conserved, the phase of these amplitudes is given by the strong $B'\pi$ scattering phase shifts in the final-state S wave (for A) or P wave (for B), i.e.,

$$A = A_0 \exp\left(i\delta_{B'\pi}^S\right), \qquad B = B_0 \exp\left(i\delta_{B'\pi}^P\right), \tag{6.2}$$

with A_0, B_0 real. Aside from the πN system, these phase shifts are not known precisely, but are estimated to be $\simeq 10°$ in magnitude. The decay rate is expressed in terms of the partial wave amplitudes by

$$\Gamma_{B \to B'\pi} = \frac{|\mathbf{q}|(E' + m_{B'})}{4\pi m_B} \left(|A|^2 + |\bar{B}|^2 \right), \tag{6.3}$$

where $\mathbf{q}$ is the pion momentum in the parent rest frame and we define $\bar{B} \equiv (E' - m_{B'}/E' + m_{B'})^{1/2} B$. Additional observables are the decay distribution $W(\theta)$,

$$W(\theta) = 1 + \alpha \mathbf{P}_B \cdot \hat{\mathbf{p}}_{B'}, \qquad \alpha = \frac{2\mathrm{Re}\,(A^* \bar{B})}{|A|^2 + |\bar{B}|^2}, \tag{6.4}$$

and the polarization $\langle \mathbf{P}_{B'} \rangle$ of the final-state baryon,

$$\langle \mathbf{P}_{B'} \rangle = \frac{(\alpha + \mathbf{P}_B \cdot \hat{\mathbf{p}}_{B'})\,\hat{\mathbf{p}}_{B'} + \beta\,(\mathbf{P}_B \times \hat{\mathbf{p}}_{B'}) + \gamma\,[\hat{\mathbf{p}}_{B'} \times (\mathbf{P}_B \times \hat{\mathbf{p}}_{B'})]}{W(\theta)},$$

$$\beta = \frac{2\mathrm{Im}(A^* \bar{B})}{|A|^2 + |\bar{B}|^2}, \qquad \gamma = \frac{|A|^2 - |\bar{B}|^2}{|A|^2 + |\bar{B}|^2} = \pm\sqrt{1 - \alpha^2 - \beta^2}, \tag{6.5}$$

where $\mathbf{P}_B$ is the polarization of B and $\hat{\mathbf{p}}_{B'}$ is a unit vector in the direction of motion of B'. Experimental studies of these distributions lead to the amplitudes listed in Table XII–5.

The nonleptonic amplitudes may be decomposed into isospin components in a notation where superscripts refer to $\Delta I = 1/2$, $3/2$,

$$
\begin{aligned}
A_{\Lambda \to p\pi^-} &= \sqrt{2}\, A_\Lambda^{(1)} - A_\Lambda^{(3)}, & A_{\Sigma^- \to n\pi^-} &= A_\Sigma^{(1)} + A_\Sigma^{(3)}, \\
A_{\Lambda \to n\pi^0} &= -A_\Lambda^{(1)} - \sqrt{2}\, A_\Lambda^{(3)}, & A_{\Sigma^+ \to n\pi^+} &= \frac{1}{3} A_\Sigma^{(1)} - \frac{2}{3} A_\Sigma^{(3)} + X_\Sigma, \\
A_{\Xi^0 \to \Lambda\pi^0} &= -A_\Xi^{(1)} - \sqrt{2}\, A_\Xi^{(3)}, & \sqrt{2}\, A_{\Sigma^+ \to p\pi^0} &= -\frac{2}{3} A_\Sigma^{(1)} + \frac{4}{3} A_\Sigma^{(3)} + X_\Sigma, \\
A_{\Xi^- \to \Lambda\pi^-} &= \sqrt{2}\, A_\Xi^{(1)} - A_\Xi^{(3)}, & &
\end{aligned}
\tag{6.6}
$$

and X_Σ is of mixed symmetry. Similar relations hold for the B amplitudes. From the entries in Table XII–5 it is not hard to see that the $\Delta I = 1/2$ rule, described previously for kaon decays, is also present here. Table XII–6 illustrates that the dominance of $\Delta I = 1/2$ amplitudes compared to those with $\Delta I = 3/2$ holds in the six possible tests in S-wave and P-wave hyperon decay, at about the same level (several per cent) as occurs in kaon decay.[9] Thus, the $\Delta I = 1/2$ rule is not an accident of kaon physics, but is rather a universal feature of nonleptonic decays. This makes the failure to clearly understand it all the more frustrating.

---

[9] For P waves, the observed smallness of $B_{\Sigma^- \to n\pi^-}$ indicates that $B_\Sigma^{(1)}$ is small, presumably accidentally so. In this case the measure of $\Delta I = 3/2$ to $\Delta I = 1/2$ effects is given by $B_\Sigma^{(3)}/X_\Sigma$.

Table XII–5. *Hyperon decay amplitudes.[a]*

Mode	A amplitudes		B amplitudes	
	Expt.	Thy.[b]	Expt.	Thy.
$\Lambda \to p\pi^-$	3.25	3.38	22.1	23.0
$\Lambda \to n\pi^0$	−2.37	−2.39	−15.8	−16.0
$\Sigma^+ \to n\pi^+$	0.13	0.00	42.2	4.3
$\Sigma^+ \to p\pi^0$	−3.27	−3.18	26.6	10.0
$\Sigma^- \to n\pi^-$	4.27	4.50	−1.44	−10.0
$\Xi^0 \to \Lambda\pi^0$	3.43	3.14	−12.3	3.3
$\Xi^- \to \Lambda\pi^-$	−4.51	−4.45	16.6	−4.7

[a] In units of 10^{-7}.
[b] Lowest-order chiral fit.

The assumption that the dominant $\Delta I = 1/2$ hamiltonian is a member of an $SU(3)$ octet leads to an additional formula, called the Lee-Sugawara relation,

$$\sqrt{3}\, A_{\Sigma^+ \to p\pi^0} = 2A_{\Xi^- \to \Lambda\pi^-} + A_{\Lambda \to p\pi^-}, \tag{6.7}$$

which also is well satisfied by the data. In this case, the corresponding formula for the B amplitudes is *not* a symmetry prediction [MaRR 69], although for unknown reasons it is in qualitative accord there also.

Lowest-order chiral analysis

Chiral symmetry provides a description of hyperon nonleptonic decay, which is of mixed success when truncated at lowest order in the energy expansion. Given our comments on the convergence of the energy expansion for baryons made in Sect. XII–3, the need for corrections to the lowest-order results is not surprising. We shall present the lowest-order analysis here, as it forms the starting point for most theoretical analyses.

Recalling from Sect. IV–7 the procedure for adding baryons to the chiral analysis, one finds that the two following nonderivative lagrangians have the chiral $(8_L, 1_R)$ transformation property:

Table XII–6. *Ratio of $\Delta I = 3/2, 1/2$ amplitudes.*

	S wave	P wave
Λ	0.014	0.006
Σ	−0.017	−0.047
Ξ	0.034	0.023
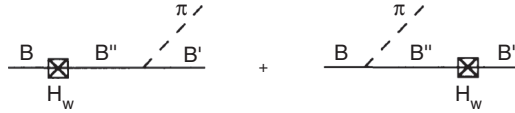
Fig. XII–1 P-wave hyperon decay amplitudes.

$$\mathcal{L}_W^{(S)} = D \operatorname{Tr} \left(\bar{B} \{ \xi^\dagger \lambda_6 \xi, B \} \right) + F \operatorname{Tr} \left(\bar{B} \left[\xi^\dagger \lambda_6 \xi, B \right] \right),$$
$$\mathcal{L}_W^{(P)} = D_5 \operatorname{Tr} \left(\bar{B} \gamma_5 \{ \xi^\dagger \lambda_6 \xi, B \} \right) + F_5 \operatorname{Tr} \left(\bar{B} \gamma_5 \left[\xi^\dagger \lambda_6 \xi, B \right] \right), \qquad (6.8)$$

where ξ, B are defined in Eqs. (3.1), (3.2) respectively. However, the operator $\mathcal{L}_W^{(P)}$ must vanish, as it has the wrong transformation property under CP [LeS 64]. That is, a CP transformation implies

$$B \to \left(i \gamma_2 \bar{B} \right)^T, \qquad \xi \to \left(\xi^\dagger \right)^T, \qquad (6.9)$$

and including the anticommutation of B and $\bar{B}$, $\mathcal{L}_W^{(S)}$ is seen to return to itself, but $\mathcal{L}_W^{(P)}$ changes sign and hence must vanish. This leaves $\mathcal{L}_W^{(S)}$ as the only allowed chiral lagrangian at lowest order. Observe that $\mathcal{L}_W^{(S)}$ lacks a γ_5 factor. Thus, its $B \to B'\pi$ matrix elements will be parity-violating, leading to only A amplitudes. The parity-conserving B amplitudes in $B \to B'\pi$ are produced through pole diagrams as in Fig. XII–1, and are proportional to the parity-conserving $B \to B'$ matrix elements of $\mathcal{L}_W^{(S)}$.

The counting of powers of energy (momentum transfer) in the energy expansion goes as follows. Both the $B \to B'$ transition and the A amplitudes in $B \to B'\pi$ are obtained as matrix elements of $\mathcal{L}_W^{(S)}$, which is zeroth order in the energy. The pole diagrams are likewise of zeroth order in the energy, being the product of the $\mathcal{L}_W^{(S)}$ vertex ($\mathcal{O}(1)$), a baryon propagator ($\mathcal{O}(q^{-1})$) and an $NN\pi$ vertex ($\mathcal{O}(q)$). Since the kinematic part of the pole diagrams, $\bar{u}'\gamma_5 u \sim \boldsymbol{\sigma} \cdot \mathbf{q}$, is of first order in q, the B amplitudes themselves are of order $B \sim q^{-1} \sim 1/\Delta m$ for the baryon pole. Kaon poles and higher-order chiral lagrangians enter at next order, i.e., having one power of the momentum transfer.

The lowest-order chiral $SU(3)$ analysis provides a fit to the data in terms of two parameters, called F and D,

$$i A_{\Lambda \to n\pi^0} = -\frac{1}{2F_\pi}(3F + D), \qquad i A_{\Sigma^+ \to p\pi^0} = \frac{\sqrt{6}}{2F_\pi}(D - F),$$
$$i A_{\Sigma^+ \to n\pi^+} = 0, \qquad\qquad\quad i A_{\Xi^0 \to \Lambda\pi^0} = \frac{1}{2F_\pi}(3F - D), \qquad (6.10)$$

with other amplitudes being predicted by the $\Delta I = 1/2$ rule. Use of the numerical values

$$\frac{D}{F} = -0.42, \qquad \frac{F}{2F_\pi} = 0.92 \times 10^{-7}, \tag{6.11}$$

leads to the excellent fit of the S-wave amplitudes seen in Table XII–5. Note that this form has one less free parameter than the general $SU(3)$ structure [MaRR 69]. Thus, the prediction of chiral symmetry that $A_{\Sigma^+ \to n\pi^+} \simeq 0$ is independent of the D/F ratio (up to $\Delta I = 3/2$ effects), and represents a successful explanation of the smallness of this amplitude.

In principle, the A amplitudes, together with the strong $BB'\pi$ vertices, determine the baryon pole contributions to the B amplitudes. These are then parametrized by the same d/f ratio as in the axial current,[10] e.g.,

$$\mathcal{M}_{\Sigma^+ \to \Sigma^+ \pi^0} = \frac{2f}{F_\pi} \bar{u} \gamma_\mu \gamma_5 u \, q^\mu = \frac{g_A^{\Sigma^+ \Sigma^+}}{F_\pi} \bar{u} \gamma_\mu \gamma_5 u \, q^\mu$$
$$= \frac{2g_{\pi NN}}{2m_N} \frac{f}{f+d} \bar{u} \gamma_\mu \gamma_5 u \, q^\mu \, . \tag{6.12}$$

Using this parameterization for the pole diagrams, one finds contributions such as

$$B_{\Sigma^+ \to p\pi^0} = -\frac{m_N + m_\Sigma}{2m_N F_\pi} \cdot \frac{(d-f)\mathcal{M}_{\Sigma^+ p}}{m_\Sigma - m_N}. \tag{6.13}$$

Taking $d + f = 1.27$, $d/f = 1.8$, one obtains from relations like this the disappointing P-wave predictions quoted in Table XII–5. This failure to simultaneously fit the S waves and P waves is a deficiency of the lowest-order chiral analysis. Perhaps this is not too surprising, as the chiral expansion converges slower in baryons than in mesons [BoH 99]. At the next order in the energy expansion, the chiral analysis contains enough free parameters to accommodate the data, but is not predictive. Lattice studies are just beginning to explore this topic [BeBPS 05].

Problems

(1) **The axial-vector coupling**

Consider the effective lagrangian in Eq. (3.1) for nucleons and pions. For combined left-handed and right-handed transformations of the fields, we have

$$U \to LUR^\dagger, \quad \xi \to L\xi V^\dagger = V\xi R^\dagger, \quad N \to VN,$$

where $L[R]$ are the spacetime independent $SU(2)$ matrices corresponding to global transformations in $SU(2)_L[SU(2)_R]$ and $V = V(\pi(x))$ is an $SU(2)$

---

[10] This statement is the $SU(3)$ generalization of the Goldberger–Treiman relation, Eqs. (3.20), (3.24).

matrix describing a vectorial transformation of the nucleons. For the lagrangian of Eq. (3.1), use Noether's theorem to generate the $SU(2)$ axial-vector current,

$$A_\mu^j = \frac{g_A}{4} \bar{\psi} \gamma_\mu \gamma_5 \left(\xi \lambda^j \xi^\dagger + \xi^\dagger \lambda^j \xi\right) \psi,$$

where ξ is the 'square root' of U (cf. Eq. (3.1)), and thereby show that the axial-vector coupling constant for beta decay is given by $g_1 = g_A$.

(2) **CP violation and nonleptonic hyperon decay**
Although the $\Delta S = 1$ hamiltonian of the Standard Model contains a *CP*-violating component, there is no *practical* way to see this in any single hyperon decay mode. Rather, one must compare the decays of hyperons with those of antihyperons [DoHP 86]. In the presence of *CP* violation, there are two sources of phases in the weak matrix elements, e.g., for the Λ decay modes,

$$A_{\Lambda \to p\pi^-} = A_1 \, e^{i\varphi_1^S} \, e^{i\delta_1^S} + A_3 \, e^{i\varphi_3^S} \, e^{i\delta_3^S},$$
$$B_{\Lambda \to p\pi^-} = B_1 \, e^{i\varphi_1^P} \, e^{i\delta_1^P} + B_3 \, e^{i\varphi_3^P} \, e^{i\delta_3^P},$$

where the isospin (I) subscripts '1, 3' stand for $\Delta I = 1/2, 3/2$, the angular momentum (J) superscripts 'S, P' stand for S waves or P waves, A_I are real amplitudes, δ_I^J are strong final-state phases, and φ_I^J are the weak *CP*-violating phases. Observe that there are three small parameters in these amplitudes – the weak phases φ_I^J, the strong phases $\delta_I^J \simeq 10°$, and the ratio of $\Delta I = 3/2$ to $\Delta I = 1/2$ effects. To leading order in these quantities, show that one has the *CP*-odd observables,

$$\frac{\beta + \overline{\beta}}{\alpha - \overline{\alpha}} = \sin\left(\varphi_1^S - \varphi_1^P\right), \qquad \frac{\alpha + \overline{\alpha}}{\alpha - \overline{\alpha}} = -\sin\left(\varphi_1^S - \varphi_1^P\right)\sin\left(\delta_1^S - \delta_1^P\right),$$

$$\frac{\Gamma_{p\pi^-} - \overline{\Gamma}_{\overline{p}\pi^+}}{\Gamma_{p\pi^-} + \overline{\Gamma}_{\overline{p}\pi^+}} = -2 \frac{A_1 A_3 \sin(\delta_1^S - \delta_3^S)\sin(\varphi_1^S - \varphi_3^S)}{|A_1|^2 + |\overline{B}_1|^2}$$
$$- 2 \frac{\overline{B}_1 \overline{B}_3 \sin(\delta_1^P - \delta_3^P)\sin(\varphi_1^P - \varphi_3^P)}{|A_1|^2 + |\overline{B}_1|^2}.$$

A hierarchy is apparent in these three signals. The $\beta + \overline{\beta}$ asymmetry requires only the weak phase, the $\alpha + \overline{\alpha}$ asymmetry requires both the weak and final-state phases, while $\Gamma - \overline{\Gamma}$ has both phases plus a $\Delta I = 3/2$ suppression. Present experiments are not sufficiently sensitive to test for *CP* violation in these observables at the required accuracy.